(Brea, CA). 3,5,3′-L-triiodothyronine (T_3) was purchased from Nacalai Tesque (Kyoto, Japan). AG-1-X8 anion exchange resin (chloride form; 200-400 mesh) was obtained from Bio-Rad (Hercules, CA). All other chemicals were of the highest purity available.

Cell Culture. Caco-2 cells at *Passage 18* obtained from the American Type Culture Collection (ATCC HTB-37) were maintained by serial passage in plastic culture dishes as described previously (12). For uptake experiments, 35-mm plastic culture dishes were inoculated with 2×10^5 cells in 2 ml of complete culture medium. The medium consisted of DMEM (Sigma) supplemented with 10% fetal bovine serum (Whittaker Bioproducts, Walkersville, MD) and 1% non-essential amino acids (Invitrogen Life Technologies, Carlsbad, CA) without antibiotics before T_3 treatment. Cells were used for experiments on the 15th day after seeding. In this study, Caco-2 cells were used between *Passages 35* and *48*.

Cell Treatment. A stock solution of T_3 was prepared as a 1 mM solution in 0.1 M NaOH. For T_3 treatment, serum was treated with anion exchange resin AG-1-X8 to remove the thyroid hormone according to the method of Samuels *et al.* (13). The T_3 concentration in the treated serum was below the level of detection (<0.15 ng/ml) of an enzyme immunoassay method (Imx; Dainabot, Tokyo, Japan). To expose the Caco-2 cell monolayers to T_3, we used a culture medium containing T_3-depleted serum and 100 nM T_3. T_3 treatment was applied to post-confluent monolayers. The control cells were incubated with the same concentration of 0.1 M NaOH in each experiment.

Measurements of Cellular Accumulation and Transcellular Transport. The cellular accumulation and transcellular transport of [^{3}H]digoxin were measured using monolayer cultures grown on 35-mm culture dishes and Transwell™ cell chambers (Costar, Cambridge, MA), respectively. The composition of the incubation medium was as follows: 145 mM NaCl, 3 mM KCl, 1 mM $CaCl_2$, 0.5 mM $MgCl_2$, 5 mM D-glucose, and 5 mM HEPES (pH 7.4).

The accumulation of [^{3}H]digoxin was studied according to the method of Ashida *et al.* (12). Radioactivity was measured in 3 ml of ACS II (Amersham Pharmacia Biotech) by liquid scintillation counting. The protein contents of cell monolayers solubilized in 1 N NaOH were determined using a Bio-Rad protein assay kit with bovine γ -globulin as the standard.

For transcellular transport experiments, after removal of the culture medium from both sides of the monolayers, the cell monolayers were preincubated with 2 ml of incubation medium at 37°C for 10 min. Then, 2 ml of incubation medium containing [^{3}H]digoxin and [^{14}C]inulin was added to either the basolateral or the apical side, with 2 ml of non-radioactive incubation medium added to the opposite side for specified periods at 37°C. After the incubation, aliquots (50 μl) of the incubation medium on the other side were taken at specified time points, and the radioactivity of [^{3}H]digoxin and [^{14}C]inulin was measured. [^{14}C]inulin was used for the correction of paracellular transport.

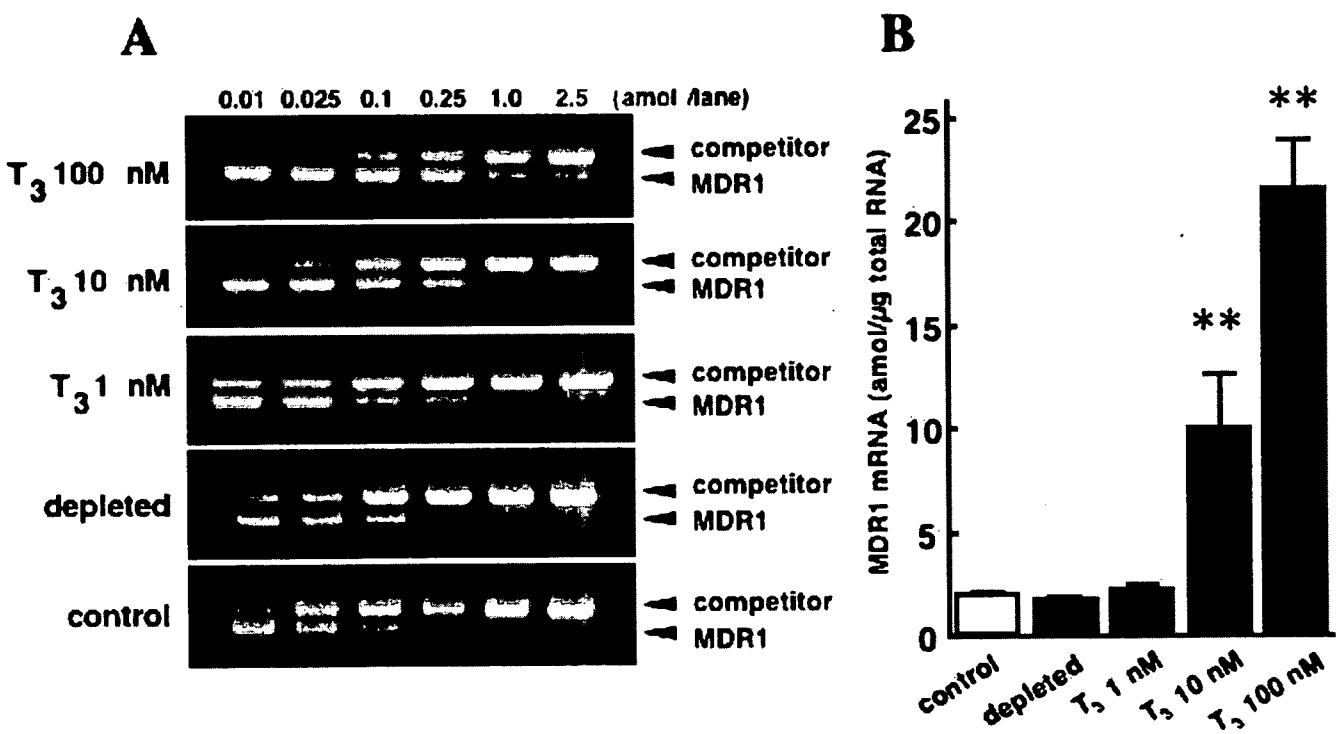

Fig. 1. Dose-dependent effects of T_3 on the expression of MDR1 mRNA in Caco-2 cells. Cells were treated with various concentrations of T_3 (depleted, 1 nM, 10 nM, 100 nM) for 3 days. Depleted represents treatment with the culture medium removed the thyroid hormone from serum by anion exchange resin AG-1-X8. After treatment, total RNA was isolated and competitive PCR was performed to determine MDR1 mRNA levels. **A** Typical results of agarose gel electrophoresis of the PCR products from T_3-treated cells. **B** Densitometric quantification of MDR1 mRNA, corrected using the amount of GAPDH mRNA as an internal control. Each column represents the mean±SE of six monolayers. *Double asterisk*, $P<0.01$, significantly different from the control.

Competitive Polymerase Chain Reaction (PCR). Competitive PCR was performed according to the method of Masuda *et al.* (14) with some modifications. Aliquots of 1 μg of total cellular RNA, isolated from Caco-2 cells using the RNeasy Mini Kit (Qiagen, Hilden, Germany), were reverse-transcribed in 20 μl of diluted reaction mixture and diluted to 200 μl. Aliquots of 5 μl of diluted reaction mixture, in combination with a semi-logarithmic serial dilution of mimic competitor DNA from 100 to 0.01 amol, were amplified by PCR according to the following method: 5 μM human MDR1 sense primer and 5 μM antisense primer in 20 μl were incubated according to the following PCR profile: an initial denaturation step of 95°C for 3 min followed by the cycling program, 95°C for 1 min, 65° C for 1 min, and 72°C for 1 min, and a final elongation step of 72°C for 10 min. For each primer set, the number of PCR cycles was increased under otherwise fixed conditions to determine the point halfway through the exponential phase. The number of cycles was 34 for MDR1. PCR products were then sized-fractionated by 1.5% agarose gel electrophoresis. The amplified cellular fragments of MDR1 were 546 bp, and the mimic competitor was 604 bp. The amount of competitor DNA yielding equal molar amounts of product gave that of the target MDR1 mRNA.

Western Blot Analysis. The apical membrane fraction from Caco-2 cells was isolated as described previously (12). After blotting onto Immobilon-P membranes (Millipore, Bedford, MA), the monoclonal antibody C219 (CIS Bio International, Gif-sur-Yvette, France) and a polyclonal antibody to villin (Santa Cruz Biotechnology, Santa Cruz, CA) were used to detect the expression of P-gp and villin, respectively. The relative densities of the bands in each lane were determined using NIH Image 1.61 (National Institutes of Health, Bethesda, MD), and the densitometric ratio of Pgp to that of villin was calculated.

Statistical Analysis. Data were analyzed statistically with a non-paired *t* test. Probability values of less than 5% were considered significant. In the mRNA analysis by Competitive PCR, statistical analysis was performed with the one-way ANOVA followed by Dunnett's post hoc testing.

RESULTS

mRNA Analysis by Competitive PCR. We used the serum treated with anion exchange resin to deplete thyroid hormone and then added various concentrations of T_3. Figure 1 shows the effect of various concentrations of T_3 (1 nM to 100 nM or depletion) on the expression of MDR1 mRNA in Caco-2 cells. The expression levels of MDR1 mRNA were increased by T_3 pretreatment for 3 days in a concentration-dependent manner.

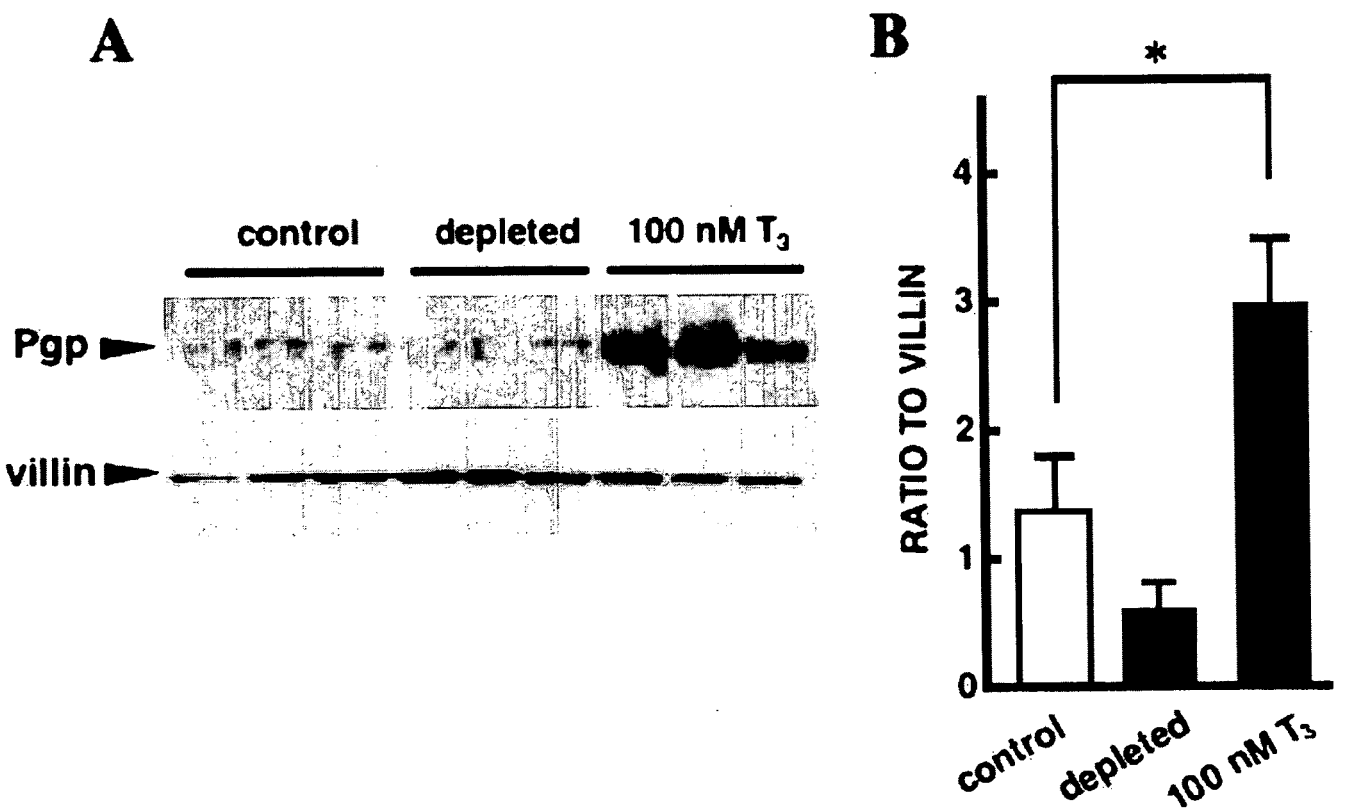

Fig. 2. Western blot analysis of the apical membranes from Caco-2 cells for Pgp. Apical membranes (50 μg) from Caco-2 cells were separated by SDS-PAGE (7.5%) and blotted onto a polyvinylidene difluoride membrane. The monoclonal antibody C219 (200 ng/ml) and a polyclonal antibody to villin (1:1,000) were used to detect the expression of Pgp and villin as primary antibodies. A horse radish peroxidase-conjugated anti-mouse IgG antibody and anti-goat IgG antibody were used for detection of bound antibodies, and strips of blots were visualized by chemiluminescence on X-ray film. **A** Immunoblotting of apical membranes from Caco-2 cells treated with 100 nM T_3 or without T_3 (depleted). **B** Densitometric quantification of Pgp. The level of C219 was corrected using villin as an internal standard. Each column represents the mean± SE of three samples. *Asterisk*, $P<0.05$, significantly different from the control.

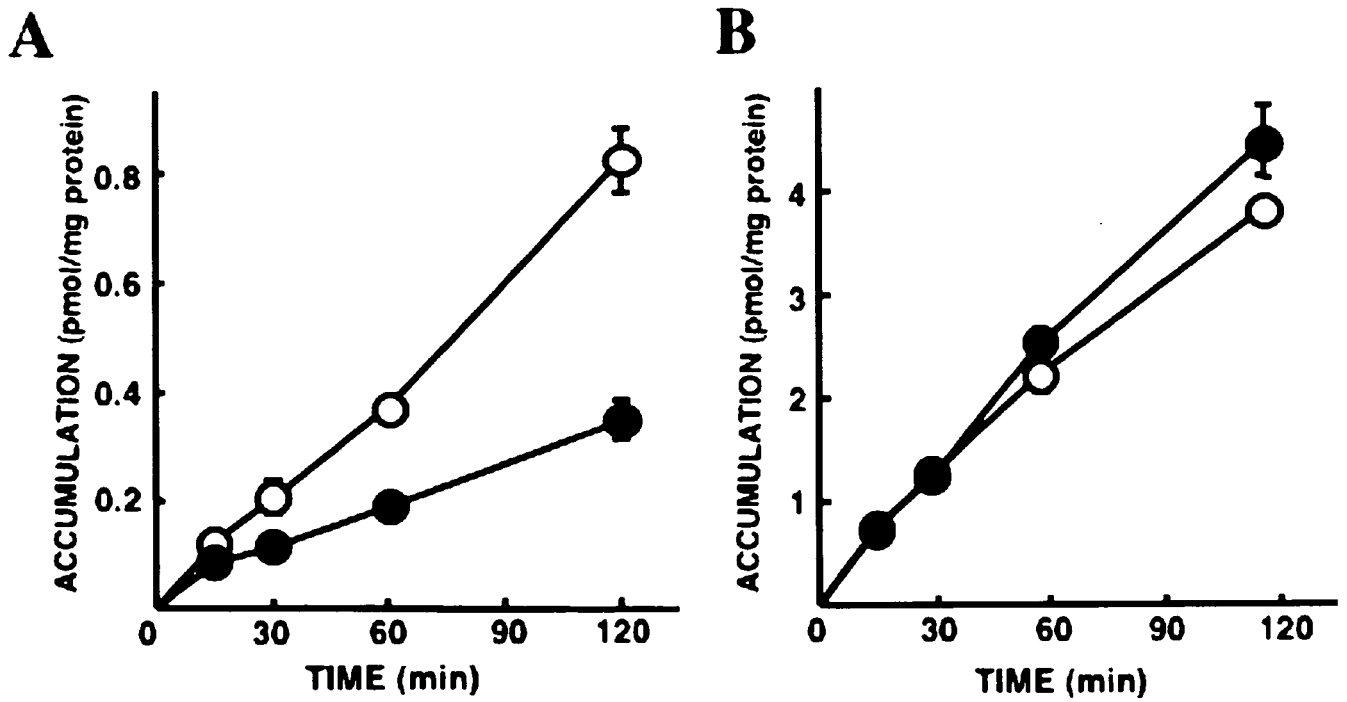

Fig. 3. Effects of T_3 on the uptake of [^{3}H]digoxin by Caco-2 cells in the **A** absence or **B** presence of 10 μM cyclosporin A. The uptake of [^{3}H]digoxin by Caco-2 cells treated with 100 nM T_3 (closed circle) or without T_3 (open circle) for 3 days was measured for specified periods at 37°C. Each point represents the mean±SE of nine monolayers from three separate experiments.

Western Blotting. Then Western blotting was performed to investigate the effect of T_3 on the expression of Pgp in Caco-2 cells (Fig. 2). A significant increase in Pgp expression was observed in Caco-2 cells pretreated with 100 nM T_3 for 3 days. In contrast, the expression level was decreased by half on the depletion of T_3.

Effect of T_3 Pretreatment on Cellular Accumulation and Transcellular Transport of [^{3}H]digoxin in Caco-2 Cells. To investigate whether the transport activity of Pgp was altered by T_3 pretreatment in Caco-2 cells, we performed [^{3}H]digoxin uptake experiments. As shown in Fig. 3, the uptake of digoxin was decreased significantly by T_3 pretreatment. In the presence of 10 μM cyclosporin A, an inhibitor of Pgp, the amount of digoxin accumulated in T_3-treated cells did not differ from that in non-pretreated cells. Figure 4 shows the transcellular transport of digoxin across Caco-2 cell monolayers. The transcellular transport of digoxin from the apical to basolateral side of Caco-2 cell monolayers treated with 100 nM T_3 was very low similar to the control. On the other hand, the basolateral to apical transcellular transport of digoxin was significantly increased across Caco-2 cell monolayers treated with 100 nM T_3. These results indicated that T_3 pretreatment caused the stimulation of Pgp-mediated transport following a significant increase in Pgp expression.

DISCUSSION

Earlier investigations suggested that the expression of Pgp varies in response to several factors. Westphal *et al.* (15) showed that treatment with rifampin resulted in an increase in the expression of duodenal Pgp and MDR1 mRNA, and Pgp expression significantly correlated with the systemic clearance of intravenous talinolol. In addition, it was reported that St John's Wort induced intestinal Pgp expression in rats

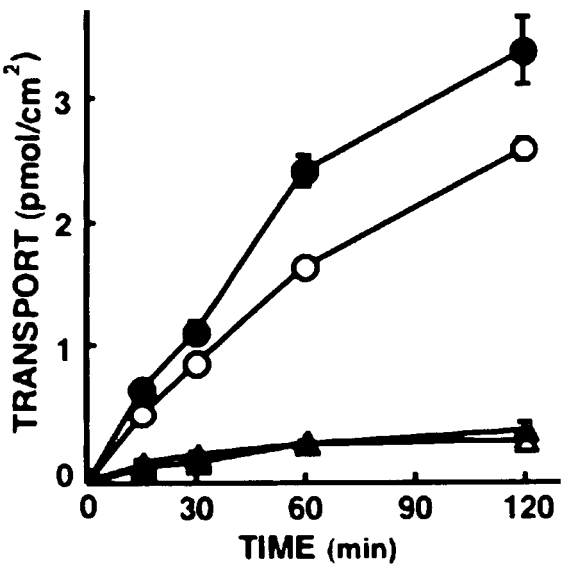

Fig. 4. Effects of T_3 on the transcellular transport of [^{3}H]digoxin using Caco-2 cells. The transcellular transport of [^{3}H]digoxin by Caco-2 cells treated with 100 nM T_3 (*closed symbol*) or without T_3 (*open symbol*) for 3 days was measured. [^{3}H]Digoxin was added to either the basolateral (*circle*) or the apical (*triangle*) side of Caco-2 cells, and incubated for specified periods at 37°C. After the incubation, the radioactivity in the medium of the opposite site was measured. Each point represents the mean±SE of nine monolayers from three separate experiments.

and humans (16). Cyclosporin A treatment also induced the expression of Pgp in the kidney and other tissues in rats (17). We previously reported that levels of Pgp and mdr1a/1b mRNA were increased in the hyperthyroid rat kidney, liver, and intestine (10). Western blot analysis revealed that Pgp expression was markedly increased in the kidney and liver of hyperthyroid rats. In contrast, it was slightly increased in the jejunum and ileum. In the present study, however, we showed that treatment with T_3 resulted in significantly increased levels of Pgp and MDR1 mRNA in Caco-2 cells. Several reports have indicated a cell type- or species-specific regulation of mdr gene expression. Zhao *et al.* showed that MDR1 mRNA levels were elevated in dexamethasone-treated $HepG_2$ cells, a human hepatoma cell line, but not in nonhepatoma HeLa cells (18). In addition, Chin *et al.* demonstrated that exposure to several drugs increased mdr RNA levels substantially in rodent cells, but not human cells (19). Thus, it is suggested that species differences exist in the susceptibility to Pgp induction. Further studies are needed to elucidate the precise mechanism of transcriptional regulation of MDR1 mRNA by thyroid hormone.

Thyroid hormones have a diverse range of actions including effects on differentiation and development, thermogenesis, and metabolism. Therefore, pathologic abnormalities in serum thyroid hormone levels result in physiological changes. For example, patients with hyperthyroidism often exhibit weight loss, a low cholesterol level, an elevated body temperature, and tachycardia, whereas hypothyroidism provokes hypercholesterolemia, myxedema, and bradycardia (20). It is known that thyroid hormone activates nuclear receptors as a ligand, leading to mRNA expression and subsequent protein synthesis. Therefore, changes in serum thyroid hormone levels may affect the expression of proteins that are of physiological importance.

Previous studies have shown that thyroid hormone affects the expression level of several membrane transporters such as the peptide transporter PEPT1 (12,21), the glucose transporter GLUT4 (22), the fructose transporter GLUT5 (23), the ATP-binding cassette transporter ABCA1 (24), Na^+, K^+-ATPase (25), and the Na^+/H^+ exchanger NHE1 (26). In addition, Siegmund *et al.* (11) showed that administration of levothyroxine tended to induce the up-regulation of MDR1 mRNA and Pgp expression in healthy volunteers. However, it did not result in major alterations in the pharmacokinetics of talinolol because their group administered levothyroxine in doses that did not cause thyrotoxicosis. In the present study, we showed that in Caco-2 monolayers treated with 100 nM T_3, the accumulation of [^{3}H]digoxin was decreased significantly and the basal-to-apical transcellular transport of [^{3}H]digoxin was accelerated compared with that in control cells. In the hypothyroid state, no change of MDR1 mRNA expression was observed compared to the control. On the other hand, the Pgp expression level decreased by half on depletion of T_3 and the amount of [^{3}H]digoxin accumulated increased slightly (1.27- to 1.50-fold). Therefore, it is possible that the mechanisms behind the regulation of Pgp expression by T_3 differ in the hyperthyroid *versus* hypothyroid.

In the present study, the altered expression of Pgp was correlated with the transport activity of digoxin in Caco-2 cells. The findings correspond to clinical reports that the blood concentration of digoxin is decreased in hyperthyroidism and increased in hypothyroidism. In contrast, there are several reports indicating the lack of pharmacokinetic alterations in the hyperthyroidism (27). For example, Ochs *et al.* (28) reported that the kinetics of diazepam were not altered in patients with hyperthyroidism. However, diazepam is not a substrate for Pgp and the metabolism by CYP2C19 and CYP3A4 are considered to be main pathways in the elimination of diazepam from the body. Therefore, it is likely that the kinetics of diazepam are not affected with hyperthyroidism. As for Pgp substrates, it was recently reported that long-term levothyroxine treatment decreased the oral bioavailability of cyclosporine A (29). Thus, it is reasonable to assume that the changes in Pgp expression in the human gut affect at least in part the alteration of the blood concentration of digoxin. Although it is impossible to investigate the changes in Pgp expression in other human tissues for ethical reasons, urinary excretion of digoxin might be increased if the expression of Pgp could be induced in the human kidney.

During the course of this study, Mitin *et al.* (30) reported that levothyroxine up-regulated the expression of Pgp mRNA and protein *in vitro*. Their observations were consistent with the present finding that treatment with T_3 resulted in the inducible expression of Pgp and MDR1 mRNA in Caco-2 cells. In addition, we further demonstrated that the basal-to-apical transcellular transport of [^{3}H]digoxin was accelerated by T_3 treatment. However, the precise molecular mechanisms underlying the induction of Pgp expression by T_3 remain to be clarified.

In conclusion, we demonstrated that thyroid hormone regulates the expression and function of Pgp. It is possible that changes in Pgp expression alter the pharmacokinetics of Pgp substrates in patients with thyroid disorders.

ACKNOWLEDGMENTS

This work was supported in part by the 21st Century COE Program "Knowledge Information Infrastructure for Genome Science", by a Grant-in-Aid for Scientific Research from the Ministry of Education, Culture, Sports, Science, and Technology of Japan, and by The Nakatomi Foundation. N. N. is supported as a Teaching Assistant by the 21st Century COE Program "Knowledge Information Infrastructure for Genome Science."

REFERENCES

1. J. H. Lin and M. Yamazaki. Role of P-glycoprotein in pharmacokinetics: clinical implications. *Clin. Pharmacokinet.* **42**:59–98 (2003).
2. B. Greiner, M. Eichelbaum, P. Fritz, H. P. Kreichgauer, O. von Richter, J. Zundler, and H. K. Kroemer. The role of intestinal P-glycoprotein in the interaction of digoxin and rifampin. *J. Clin. Invest.* **104**:147–153 (1999).
3. M. Demeule, J. Jodoin, E. Beaulieu, M. Brossard, and R. Beliveau. Dexamethasone modulation of multidrug transporters in normal tissues. *FEBS Lett.* **442**:208–214 (1999).
4. S. Micuda, L. Mundlova, J. Mokry, J. Osterreicher, J. Cermanova, D. Cizkova, and J. Martinkova. The effect of mdr1 induction on the pharmacokinetics of rhodamine 123 in rats. *Basic Clin. Pharmacol. Toxicol.* **96**:257–258 (2005).
5. P. G. Wells, J. Feely, G. R. Wilkinson, and A. J. Wood. Effect of thyrotoxicosis on liver blood flow and propranolol disposition after long-term dosing. *Clin. Pharmacol. Ther.* **33**:603–608 (1983).

6. J. R. Lawrence, D. J. Sumner, W. J. Kalk, W. A. Ratcliffe, B. Whiting, K. Gray, and M. Lindsay. Digoxin kinetics in patients with thyroid dysfunction. *Clin. Pharmacol. Ther.* **22**:7–13 (1977).
7. G. M. Shenfield, J. Thompson, and D. B. Horn. Plasma and urinary digoxin in thyroid dysfunction. *Eur. J. Clin. Pharmacol.* **12**:437–443 (1977).
8. J. Bonelli, H. Haydl, K. Hruby, and G. Kaik. The pharmacokinetics of digoxin in patients with manifest hyperthyroidism and after normalization of thyroid function. *Int. J. Clin. Pharmacol. Biopharm.* **16**:302–306 (1978).
9. G. M. Shenfield. Influence of thyroid dysfunction on drug pharmacokinetics. *Clin. Pharmacokinet.* **6**:275–297 (1981).
10. N. Nishio, T. Katsura, K. Ashida, M. Okuda, and K. Inui. Modulation of P-glycoprotein expression in hyperthyroid rat tissues. *Drug Metab. Dispos.* **33**:1584–1587 (2005).
11. W. Siegmund, S. Altmannsberger, A. Paneitz, U. Hecker, M. Zschiesche, G. Franke, W. Meng, R. Warzok, E. Schroeder, B. Sperker, B. Terhaag, I. Cascorbi, and H. K. Kroemer. Effect of levothyroxine administration on intestinal P-glycoprotein expression: consequences for drug disposition. *Clin. Pharmacol. Ther.* **72**:256–264 (2002).
12. K. Ashida, T. Katsura, H. Motohashi, H. Saito, and K. Inui. Thyroid hormone regulates the activity and expression of the peptide transporter PEPT1 in Caco-2 cells. *Am. J. Physiol. Gastrointest. Liver Physiol.* **282**:G617–623 (2002).
13. H. H. Samuels, F. Stanley, and J. Casanova. Depletion of L-3,5,3′-triiodothyronine and L-thyroxine in euthyroid calf serum for use in cell culture studies of the action of thyroid hormone. *Endocrinology* **105**:80–85 (1979).
14. S. Masuda, S. Uemoto, T. Hashida, Y. Inomata, K. Tanaka, and K. Inui. Effect of intestinal P-glycoprotein on daily tacrolimus trough level in a living-donor small bowel recipient. *Clin. Pharmacol. Ther.* **68**:98–103 (2000).
15. K. Westphal, A. Weinbrenner, M. Zschiesche, G. Franke, M. Knoke, R. Oertel, P. Fritz, O. von Richter, R. Warzok, T. Hachenberg, H. M. Kauffmann, D. Schrenk, B. Terhaag, H. K. Kroemer, and W. Siegmund. Induction of P-glycoprotein by rifampin increases intestinal secretion of talinolol in human beings: a new type of drug/drug interaction. *Clin. Pharmacol. Ther.* **68**:345–355 (2000).
16. D. Durr, B. Stieger, G. A. Kullak-Ublick, K. M. Rentsch, H. C. Steinert, P. J. Meier, and K. Fattinger. St John's Wort induces intestinal P-glycoprotein/MDR1 and intestinal and hepatic CYP3A4. *Clin. Pharmacol. Ther.* **68**:598–604 (2000).
17. L. Jette, E. Beaulieu, J. M. Leclerc, and R. Beliveau. Cyclosporin A treatment induces overexpression of P-glycoprotein in the kidney and other tissues. *Am. J. Physiol.* **270**:F756–765 (1996).
18. J. Y. Zhao, M. Ikeguchi, T. Eckersberg, and M. T. Kuo. Modulation of multidrug resistance gene expression by dexamethasone in cultured hepatoma cells. *Endocrinology* **133**:521–528 (1993).
19. K. V. Chin, S. S. Chauhan, I. Pastan, and M. M. Gottesman. Regulation of mdr RNA levels in response to cytotoxic drugs in rodent cells. *Cell Growth Differ.* **1**:361–365 (1990).
20. R. C. Ribeiro, J. W. Apriletti, B. L. West, R. L. Wagner, R. J. Fletterick, F. Schaufele, and J. D. Baxter. The molecular biology of thyroid hormone action. *Ann. N. Y. Acad. Sci.* **758**:366–389 (1995).
21. K. Ashida, T. Katsura, H. Saito, and K. Inui. Decreased activity and expression of intestinal oligopeptide transporter PEPT1 in rats with hyperthyroidism *in vivo*. *Pharm. Res.* **21**:969–975 (2004).
22. C. J. Torrance, J. E. Devente, J. P. Jones, and G. L. Dohm. Effects of thyroid hormone on GLUT4 glucose transporter gene expression and NIDDM in rats. *Endocrinology* **138**:1204–1214 (1997).
23. M. Matosin-Matekalo, J. E. Mesonero, T. J. Laroche, M. Lacasa, and E. Brot-Laroche. Glucose and thyroid hormone co-regulate the expression of the intestinal fructose transporter GLUT5. *Biochem. J.* **339**:233–239 (1999).
24. J. Huuskonen, M. Vishnu, C. R. Pullinger, P. E. Fielding, and C. J. Fielding. Regulation of ATP-binding cassette transporter A1 transcription by thyroid hormone receptor. *Biochemistry* **43**: 1626–1632 (2004).
25. R. A. Giannella, J. Orlowski, M. L. Jump, and J. B. Lingrel. Na^+-K^+-ATPase gene expression in rat intestine and Caco-2 cells: response to thyroid hormone. *Am. J. Physiol.* **265**:G775–782 (1993).
26. X. Li, A. J. Misik, C. V. Rieder, R. J. Solaro, A. Lowen, and L. Fliegel. Thyroid hormone receptor α_1 regulates expression of the Na^+/H^+ exchanger (NHE1). *J. Biol. Chem.* **277**:28656–28662 (2002).
27. P. O'Connor and J. Feely. Clinical pharmacokinetics and endocrine disorders. Therapeutic implications. *Clin. Pharmacokinet.* **13**:345–364 (1987).
28. H. R. Ochs, D. J. Greenblatt, H. J. Kaschell, U. Klehr, M. Divoll, and D. R. Abernethy. Diazepam kinetics in patients with renal insufficiency or hyperthyroidism. *Br. J. Clin. Pharmacol.* **12**:829–832 (1981).
29. M. Jin, T. Shimada, M. Shintani, K. Yokogawa, M. Nomura, and K. Miyamoto. Long-term levothyroxine treatment decreases the oral bioavailability of cyclosporin A by inducing P-glycoprotein in small intestine. *Drug Metab. Pharmacokinet.* **20**:324–330 (2005).
30. T. Mitin, L. L. von Moltke, M. H. Court, and D. J. Greenblatt. Levothyroxine up-regulates P-glycoprotein independent of the pregnane X receptor. *Drug Metab. Dispos.* **32**:779–782 (2004).

0090-9556/08/3604-649–654$20.00
DRUG METABOLISM AND DISPOSITION
Vol. 36, No. 4
19869/3314947
Printed in U.S.A.

DMD 36:649–654, 2008

Altered Pharmacokinetics of Cationic Drugs Caused by Down-Regulation of Renal Rat Organic Cation Transporter 2 (*Slc22a2*) and Rat Multidrug and Toxin Extrusion 1 (*Slc47a1*) in Ischemia/Reperfusion-Induced Acute Kidney Injury

Takanobu Matsuzaki, Takafumi Morisaki, Wakako Sugimoto, Koji Yokoo, Daisuke Sato, Hiroshi Nonoguchi, Kimio Tomita, Tomohiro Terada, Ken-ichi Inui, Akinobu Hamada, and Hideyuki Saito

Department of Pharmacy, Kumamoto University Hospital, Kumamoto, Japan (T.Ma., T.Mo., W.S., K.Y., D.S., A.H., H.S.); Department of Nephrology, Kumamoto University Graduate School of Medical Sciences, Kumamoto, Japan (H.N., K.T.); and Department of Pharmacy, Kyoto University Hospital, Kyoto, Japan (T.T., K.I.)

Received November 21, 2007; accepted January 2, 2008

ABSTRACT:

In the proximal tubules of rat (r) kidney, the polyspecific organic cation transporters (OCTs), rOCT1 and rOCT2, mediate the basolateral uptake of various organic cations, including many drugs, toxins, and endogenous compounds, and the apical type of H^+/organic cation antiporter, rat multidrug and toxin extrusion 1 (rMATE1), mediate the efflux of organic cations. Renal clearances of H_2 receptor antagonists, including famotidine, were reported to be decreased in patients with kidney disease. Therefore, acute kidney injury (AKI) could influence renal excretion and disposition of organic cations accompanied by the regulation of organic cation transporters. The aim of this study was to investigate the pharmacokinetic alteration of cationic drugs and the expression of tubular organic cation transporters, rOCT1, rOCT2, and rMATE1, in ischemia/reperfusion (I/R)-induced AKI rats. I/R-induced AKI increased the plasma concentration of i.v. administrated famotidine, a substrate for rOCT1 and rOCT2, or tetraethylammonium (TEA), a substrate for rOCT1, rOCT2, and rMATE1. The areas under the plasma concentration curves for famotidine and TEA were 2- and 6-fold higher in I/R rats than in sham-operated rats, respectively. The accumulation of TEA into renal slices was significantly decreased, suggesting that organic cation transport activity at the basolateral membranes was reduced in I/R rat kidney. The protein expressions of basolateral rOCT2 and luminal rMATE1 were down-regulated in I/R rat kidneys. These data suggest that the urinary secretion of cationic drugs via epithelial organic cation transporters is decreased in AKI.

The kidney mediates urinary excretion of a wide variety of xenobiotics, including drugs, toxins, and endogenous compounds. In renal proximal tubules, several directional organic solute transport systems facilitate active secretion of a wide range of exogenous and endogenous organic ions (Pritchard and Miller, 1996; Inui et al., 2000). Transport proteins for organic anions and cations localized specifically at the apical or basolateral membranes of the proximal tubular cells are responsible for urinary secretion of diverse drugs (Sweet and Pritchard, 1999; Inui et al., 2000; Sekine et al., 2000). The structures and functions of *SLC22A* gene family members of organic anion transporters (OATs) and organic cation transporters (OCTs), which mediate transepithelial transport of various organic anions and cations, have been characterized (Sweet and Pritchard, 1999; Inui et al., 2000; Sekine et al., 2000). rOAT1 (*Slc22a6*) and rOAT3 (*Slc22a8*) appear to mediate organic anion/α-ketoglutarate exchange at the basolateral membrane of the proximal tubules, including various organic anions (Sekine et al., 1997; Sweet and Pritchard, 1999; Tojo et al., 1999; Cha et al., 2001). On the other hand, rOCT1 (*Slc22a1*) and rOCT2 (*Slc22a2*) were reported to be driven by inside-negative membrane potential (Busch et al., 1996; Okuda et al., 1996), mediating basolateral uptake of diverse organic cations such as tetraethylammonium (TEA) and the H_2-receptor antagonist cimetidine (Urakami et al., 2001). The H^+/organic cation antiporter in renal brush-border membranes mediates active extrusion of cationic drugs or toxins out of renal tubular cells (Ullrich, 1997). The oppositely directed H^+ gradient was demonstrated to be a driving force for the transport of organic cations such as TEA, a prototype substrate (Takano et al., 1984). More recently, the apical type of H^+/organic cation antiporter, rat multidrug and toxin extrusion 1 (rMATE1/*Slc47a1*), has been identified and functionally characterized (Ohta et al., 2006; Terada et

This work was supported in part by Grant-in-Aid for Scientific Research (B) 17390158 from the Scientific Fund of the Ministry of Education, Science, and Culture of Japan.

Article, publication date, and citation information can be found at http://dmd.aspetjournals.org.

doi:10.1124/dmd.107.019869.

ABBREVIATIONS: OAT, organic anion transporter; OCT, organic cation transporter; r, rat; TEA, tetraethylammonium; MATE, multidrug and toxin extrusion; AKI, acute kidney injury; I/R, ischemia/reperfusion; h, human; BUN, blood urea nitrogen; SCr, serum creatinine; HPLC, high performance liquid chromatography; AUC, area under the plasma concentration curve; PCR, polymerase chain reaction; NHE, Na^+/H^+ exchanger.

al., 2006). rMATE1 is expressed mainly in the kidney and placenta and is considered to be responsible for the final step of urinary excretion of cationic drugs (Terada et al., 2006). Therefore, the functional and molecular variations of these transporters under renal diseases have a great impact on renal clearance of their substrates.

Acute kidney injury (AKI) caused by ischemia/reperfusion (I/R) is a critical syndrome associated with high mortality in humans (Thadhani et al., 1996; Star, 1998; Schrier et al., 2004). I/R-induced AKI is evoked by a complicated interaction among renal hemodynamics, inflammatory cytokines, and tubular cell damages (Bonventre and Weinberg, 2003). AKI is characterized principally by tubular dysfunction with impaired sodium and water reabsorption, which are associated with the shedding and excretion of renal brush-border membranes and epithelial tubule cells into the urine (Thadhani et al., 1996). After I/R, morphological changes occur in the proximal tubules, including loss of polarity, loss of the brush border, and redistribution of integrins and Na^+/K^+-ATPase to the apical membrane (Molitoris et al., 1992; Thadhani et al., 1996; Schrier et al., 2004). Therefore, renal tubular secretion of xenobiotics and endogenous toxins could be also affected by AKI, as this important secretory process is performed by several transporting systems localized in the renal tubular cells. In patients with renal diseases, it was reported that the plasma elimination and renal clearance of the H_2 receptor antagonist famotidine were decreased compared with those in healthy volunteers (Manlucu et al., 2005). Famotidine is eliminated mainly by the kidney as the intact form by tubular secretion in addition to glomerular filtration (Lin, 1991). Famotidine was reported to be transported by the rat and human OAT family members rOAT3 and hOAT3, and the OCT family members rOCT1, rOCT2, and hOCT2 (Tahara et al., 2005). Taking these findings into consideration, we hypothesized that decreased renal excretion of famotidine in patients with renal diseases could be caused by the decreased expression and function of OAT and/or OCT family members in the kidney. We reported that renal organic anion transport activity at the basolateral membranes was suppressed in rats with I/R-induced AKI, which was accompanied by down-regulation of both rOAT1 and rOAT3 (Matsuzaki et al., 2007). In contrast, there is little information concerning the regulation of renal OCT family members in AKI. Previously, it was reported that the transport activity of organic cations in renal brush-border membranes was decreased in I/R rats (Maeda et al., 1993). However, there is no information regarding the expression of luminal rMATE1 in association with AKI. In the present study, we examined the pharmacokinetics of cationic drugs and the expression levels of tubular organic cation transporters in I/R-induced AKI rats.

Materials and Methods

Materials. [1-^{14}C]Tetraethylammonium bromide (118.4 MBq/mmol) and D-[1-^{3}H(N)]mannitol (525.4 GBq/mmol) were obtained from PerkinElmer Life and Analytical Sciences (Boston, MA). The radiochemical purity of these products was greater than 97% as guaranteed by the company. Famotidine was obtained from Wako Pure Chemicals (Osaka, Japan). All other chemicals used were of the highest purity available.

Experimental Animals. Male Sprague-Dawley rats, initially weighing 200 to 210 g (Clea Japan, Inc., Tokyo, Japan), were housed in a standard animal maintenance facility at constant temperature (21–23°C) and humidity (50–70%) with a 12-h light/dark cycle for at least 1 week before the day of the experiment. Our protocol of animal experiments was approved by the committee of the Kumamoto University Institute of Resource Development and Analysis.

Rats were anesthetized using sodium pentobarbital (50 mg/kg i.p.) and placed on a heating plate (39°C) to maintain a constant temperature. The kidneys were exposed via midline abdominal incisions. Renal ischemia was induced using vascular clamps (A.S. One Company Ltd., Osaka, Japan) over both pedicles for 30 min. After the clamps were released, the incision was closed in two layers with 3-0 sutures. Sham-operated animals underwent anesthesia, laparotomy, and renal pedicle dissection only. All animals received warm saline solution instilled in the peritoneal cavity during the surgical procedure and were then allowed to recover with ad libitum access to food and water. All experiments were performed under surgical anesthesia at 48 h after I/R. Twenty-two of 27 rats survived 48 h after surgery. Blood samples were collected for measurement of blood urea nitrogen (BUN) and serum creatinine (SCr). BUN and SCr in serum were measured at the SRL laboratory (Tokyo, Japan).

Measurement of Plasma Concentration of Famotidine. At 48 h after I/R, famotidine was administered i.v. to rats at 20 mg/kg via the left jugular vein for 1 min. Blood samples (0.4 ml) were collected from the right jugular vein at 5, 15, 30, 60, 120, and 240 min after the injection, and plasma samples were obtained by centrifugation. Urine was also collected for 240 min after injection for determining urinary recovery. The concentration of famotidine in plasma and urine was measured by high-performance liquid chromatography (HPLC). A 100-μl sample of plasma or urine was deproteinized by adding 0.2 ml of methanol and 0.1 ml of the mobile phase and centrifuged at 6000g for 10 min; 10 μl of the supernatant was injected into HPLC. The HPLC system consisted of an LC-10ADVP pump (Shimadzu, Kyoto, Japan), an SPD-10AVP ultraviolet spectrophotometric detector (Shimadzu), and a column of TSK-gel ODS 80TM (4.6 mm i.d., 150 mm length; Tosoh, Tokyo, Japan). The mobile phase consisted of a mixture of 30 mM phosphate buffer (pH 7.0) and acetonitrile (95:5, v/v), and the flow rate was 1.0 ml/min at a column temperature of 40°C. Ultraviolet absorbance was determined at a wavelength of 280 nm. Standard curves for famotidine were prepared over a range of 0.25 to 100 μg/ml and shown to be linear. The coefficients of variation for the desired concentration (2.5, 25, and 100 μg/ml) ranged from 1.4 to 3.9%. The limit of quantification was 0.25 μg/ml. Blank plasma and urine samples showed no interference with the peak corresponding to famotidine.

Measurement of Plasma and Kidney Concentrations of TEA. At 48 h after I/R, [^{14}C]TEA was administered i.v. to rats at 1.0 mg/kg via the left jugular vein for 1 min. Blood samples (0.4 ml) were collected from the right jugular vein at 5, 15, 30, 60, 120, and 240 min after the injection, and plasma samples were obtained by centrifugation. Urine was also collected for 240 min after injection for determining urinary recovery. At 240 min after injection, kidneys were collected immediately after rats were sacrificed. The excised kidneys were gently washed and weighed. Then 100-μl homogenates of plasma, urine, or kidney were solubilized in 0.5 ml of NCSII (GE Healthcare Bio-Sciences, Piscataway, NJ), and the radioactivity was determined in a liquid scintillation counter after addition of 5 ml of OCS (GE Healthcare Bio-Sciences).

Pharmacokinetic Analysis. A conventional two-compartment model was used to analyze the plasma concentration-time profiles of famotidine and TEA after i.v. administration in rats. The areas under the plasma concentration-time curves (AUCs) for famotidine and TEA were determined by the trapezoidal rule with extrapolation to infinity. Pharmacokinetic parameters calculated using standard formulae were central volume of distribution (V_1), volume of distribution at steady state (V_{ss}), plasma elimination rate constant (k_{el}), α-phase half-life ($t_{1/2\alpha}$), β-phase half-life ($t_{1/2\beta}$), total body clearance (CL_{tot}), and renal clearance (CL_{ren}).

Uptake by Rat Renal Slices. Uptake studies in isolated rat renal slices were performed as described in a previous report (Matsuzaki et al., 2007). Briefly, 12 to 15 slices prepared from the whole kidney of sham-operated and ischemic rats (n = 3) were stored in ice-cold oxygenated incubation buffer composed of 120 mM NaCl, 16.2 mM KCl, 1 mM $CaCl_2$, 1.2 mM $MgSO_4$, and 10 mM NaH_2PO_4/Na_2HPO_4 (pH 7.5). Renal slices were randomly selected and incubated in flasks containing 6 ml of the incubation buffer with [^{14}C]TEA (5 μM, 0.56 kBq/ml). The uptake of these compounds was measured at 37°C under an atmosphere of 100% oxygen. [^{3}H]Mannitol (5 μM, 1.85 kBq/ml) was used to calculate the extracellular trapping and nonspecific uptake of [^{14}C]TEA as well as to evaluate the viability of slices. After incubation for a specified period, the incubation buffer containing radiolabeled compounds was rapidly removed from the flask, and the renal slices were washed twice with 5 ml of ice-cold phosphate-buffered saline, blotted on filter paper, weighed, and solubilized in 0.5 ml of NCSII. The amount of radioactivity was then determined in a liquid scintillation counter after addition of 5 ml of OCS.

Western Blot Analysis. Kidneys (n = 3) were homogenized in homogenization buffer consisting of 230 mM sucrose, 5 mM Tris-HCl (pH 7.5), 2 mM

TABLE 1

Renal functional data at 48 h after I/R

Each value represents the mean ± S.D. from 17 to 18 rats.

	Sham	I/R
Body weight (g)	210.6 ± 8.3	190.3 ± 9.2***
BUN (mg/dl)	18.7 ± 4.9	188.9 ± 47.1***
SCr (mg/dl)	0.20 ± 0.03	2.83 ± 1.30***

***$P < 0.001$ versus sham-operated rats.

EDTA, 0.1 mM phenylmethanesulfonyl fluoride, 1 mg/ml leupeptin, and 1 mg/ml pepstatin A. After measurement of the protein content using bicinchoninic acid protein assay reagent (Pierce Chemical, Rockford, IL), each sample (40 μg) was mixed in loading buffer (2% SDS, 125 mM Tris-HCl, 20% glycerol, and 5% 2-mercaptoethanol) and heated at 100°C for 2 min. The samples were separated by 7.5% SDS-polyacrylamide gel electrophoresis and transferred onto polyvinylidene difluoride membranes (Immobilon-P; Millipore Corporation, Bedford, MA) by semidry electroblotting. The blots were blocked overnight at 4°C with 2% ECL Advance Blocking Agent (GE Healthcare Bio-Sciences) in Tris-buffered saline containing 0.3% Tween 20 (TBS-T) and incubated for 1 h at room temperature with primary antibody specific for rOCT1 (Ji et al., 2002), rOCT2 (Ji et al., 2002), rOAT1 (Matsuzaki et al., 2007), rOAT3 (Matsuzaki et al., 2007), rMATE1 (Nishihara et al., 2007), or β-actin (Sigma-Aldrich, St. Louis, MO). The blots were washed with TBS-T and incubated with the secondary antibody [horseradish peroxidase-linked anti-rabbit immunoglobulin $F(ab)_2$ or horseradish peroxidase-linked anti-mouse immunoglobulin $F(ab)_2$; GE Healthcare Bio-Sciences] for 1 h at room temperature. Immunoblots were visualized with an ECL system (ECL Advance Western Blotting Detection Kit; GE Healthcare Bio-Sciences). The relative amount of each band was determined densitometrically using Densitograph Imaging Software (ATTO Corporation, Tokyo, Japan). Densitometric ratios relative to sham-operated rats were used as the reference and accorded an arbitrary value of 100.

Real-Time PCR Analysis. The isolation of mRNA from kidney and reverse transcription were performed as described previously (Matsuzaki et al., 2007). We performed a TaqMan quantitative real-time RT-PCR using an ABI PRISM 7900 sequence detection system (Applied Biosystems, Foster City, CA) to determine the mRNA expression level of rOCT1, rOCT2, rOAT1, rOAT3, rMATE1, and eukaryotic 18S rRNA. The following TaqMan 18S rRNA control reagents and products of TaqMan Gene Expression Assays were purchased from Applied Biosystems: rOCT1, Rn00562250_m1; rOCT2, Rn00580893_m1; rOAT1, Rn00568143_m1; rOAT3, Rn00580082_m1; rMATE1, Rn01497159_m1; and 18S rRNA, 4319413E.

Statistical Analysis. Statistical significance was determined by Student's *t* test. $P < 0.05$ was considered statistically significant.

Results

Renal Functional Data for I/R-Induced AKI Rats. Renal function was first examined in rats with renal I/R. As summarized in Table 1, the body weights were slightly yet significantly decreased in I/R rats. The levels of both BUN and SCr were significantly elevated in I/R rats compared with sham-operated rats, indicating that AKI was evoked by I/R treatment.

Effects of I/R-Induced AKI on Famotidine Pharmacokinetics. To examine whether the renal disposition of famotidine is decreased in I/R rats in comparison with that in sham-operated rats, we assessed the pharmacokinetics of famotidine. The plasma concentration-time profile of famotidine up to 240 min after i.v. administration is shown in Fig. 1. The plasma concentration of famotidine in I/R rats was higher than that in sham-operated rats. Table 2 summarizes the pharmacokinetic parameters of famotidine in sham-operated and I/R rats. The AUC for famotidine in I/R rats was 2-fold higher than that in sham-operated rats. The CL_{tot} and CL_{ren} values for famotidine in I/R rats were significantly decreased to 49 and 14%, respectively, of the corresponding values in sham-operated rats. The $t_{1/2\beta}$ of famotidine

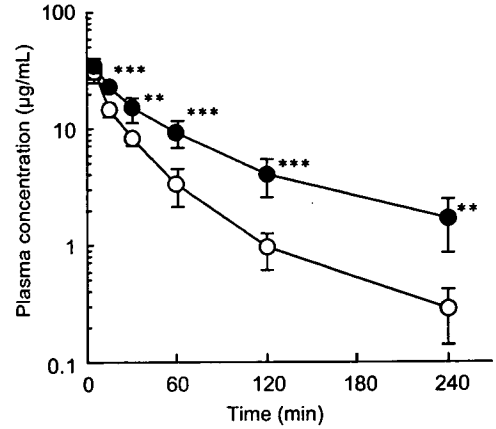

FIG. 1. Plasma concentration versus time profiles for famotidine in sham-operated (○) and I/R rats (●) after i.v. administration of famotidine (20 mg/kg). Each point represents the mean ± S.D. from six rats. **, $p < 0.01$; ***, $p < 0.001$ versus sham-operated rats.

TABLE 2

Pharmacokinetic parameters of famotidine in sham-operated and I/R rats

Each value represents the mean ± S.D. from six rats.

	Sham	I/R
Dose excreted in urine (%)	67.3 ± 7.5	18.1 ± 14.6***
AUC (μg · min/ml)	911 ± 94	1925 ± 406***
V_1 (ml/kg)	428 ± 157	424 ± 109
V_{ss} (ml/kg)	801 ± 168	810 ± 223
CL_{tot} (ml/min/kg)	22.1 ± 2.3	10.7 ± 2.0***
CL_{ren} (ml/min/kg)	14.9 ± 2.4	2.1 ± 1.8***
k_{el} (min^{-1})	0.058 ± 0.021	0.026 ± 0.007***
$t_{1/2\alpha}$ (min)	6.7 ± 3.2	7.0 ± 4.2
$t_{1/2\beta}$ (min)	38.8 ± 13.2	64.0 ± 19.7*

*$P < 0.05$ versus sham-operated rats.
***$P < 0.001$.

was significantly prolonged in I/R rats compared with that in sham-operated rats, whereas there were no significant differences in the $t_{1/2\alpha}$ of famotidine between the sham-operated and I/R rats.

Effects of I/R-Induced AKI on TEA Pharmacokinetics. We next examined the pharmacokinetics of TEA, a typical cationic substrate for rOCT1 and rOCT2. The plasma concentration-time profile of TEA up to 240 min after i.v. administration is depicted in Fig. 2A, and the pharmacokinetic parameters of TEA are summarized in Table 3. I/R caused significant changes in the pharmacokinetic behavior of TEA. The AUC for TEA was markedly elevated in I/R rats compared with that in sham-operated rats, whereas the CL_{tot} for TEA was significantly decreased in I/R rats. The AUC for TEA was almost 7-fold higher in I/R rats than that in sham-operated rats. The CL_{tot} and CL_{ren} values for TEA in I/R rats were significantly decreased to 20 and 14%, respectively, of the values in sham-operated rats. The $t_{1/2\beta}$ of TEA in I/R rats was almost 4-fold higher than that in sham-operated rats, whereas the $t_{1/2\alpha}$ of TEA was not affected.

Figure 2, B and C, shows the kidney concentrations and tissue-to-plasma concentration ratio (apparent Kp) for TEA in sham-operated and I/R rats at 240 min after i.v. administration. The concentration of TEA in the kidney was significantly elevated in I/R rats compared with that in sham-operated rats. The Kp value in I/R rat kidneys was significantly decreased to 20% of that in sham-operated rats.

Uptake of TEA by Renal Slices. To evaluate organic cation transport activity in the renal basolateral membrane, we measured the accumulation of TEA in renal slices prepared from sham-operated and I/R rat kidneys. As illustrated in Fig. 3, the accumulation of TEA was significantly lower in the I/R rats at each time point. The accumulation

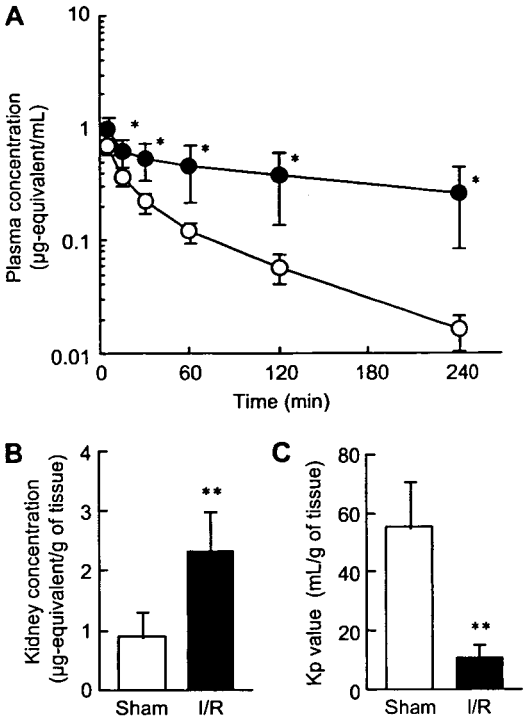

FIG. 2. A, plasma concentration versus time profiles for TEA in sham-operated (○) and I/R rats (●) after i.v. administration of [^{14}C]TEA (1.0 mg/kg). Kidney concentration (B) and tissue-to-plasma concentration ratio (Kp) value (C) of TEA in sham-operated (□) and I/R rats (■) at 240 min after i.v. administration of [^{14}C]TEA (1.0 mg/kg). Each point or column represents the mean ± S.D. from four rats. *, $p < 0.05$; **, $p < 0.01$ versus sham-operated rats.

TABLE 3

Pharmacokinetic parameters of TEA in sham-operated and I/R rats

Each value represents the mean ± S.D. from four rats.

	Sham	I/R
Dose excreted in urine (%)	78.0 ± 16.2	48.2 ± 21.6
AUC (μg · min/ml)	29.3 ± 5.8	198.0 ± 134.9*
V_1 (ml/kg)	977 ± 133	714 ± 295
V_{ss} (ml/kg)	2313 ± 374	1813 ± 547
CL_{tot} (ml/min/kg)	35.3 ± 8.1	7.1 ± 4.5**
CL_{ren} (ml/min/kg)	27.6 ± 9.3	3.8 ± 3.8**
k_{el} (min^{-1})	0.036 ± 0.005	0.010 ± 0.003***
$t_{1/2\alpha}$ (min)	6.6 ± 0.2	5.9 ± 3.7
$t_{1/2\beta}$ (min)	60.1 ± 8.1	221.3 ± 69.1**

*$P < 0.05$ versus sham-operated rats.
**$P < 0.01$.
***$P < 0.001$.

of TEA into renal slices at 60 min was significantly decreased to 36% of those in sham-operated rats.

Protein and mRNA Expression of rOCTs in I/R-Induced AKI Rats. To get precise information about the decreases in accumulation of TEA in renal slices of I/R rat kidney, we measured renal rOCT1 and rOCT2 expression using Western blot analyses. As is evident in Fig. 4, rOCT2 protein expression was markedly suppressed in I/R rat kidney compared with that in sham-operated rat kidney, whereas there was no significant difference in the expression of rOCT1. The expressions of rOAT1 and rOAT3 protein were significantly depressed in I/R rat kidney, consistent with our previous report (Matsuzaki et al., 2007).

Next, we examined mRNA expression levels of organic cation transporters, rOCT1 and rOCT2, in the kidney (Fig. 4). Compared with sham-operated rat kidneys, the levels of rOCT1 and rOCT2

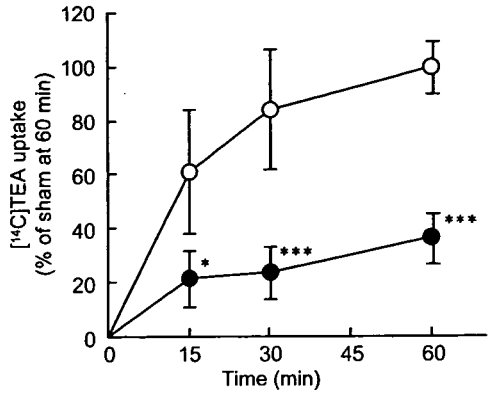

FIG. 3. Uptake of TEA in renal slices of sham-operated and I/R rats. Renal slices from sham-operated (○) and I/R rats (●) were incubated at 37°C in incubation buffer containing 5 μM [^{14}C]TEA, for the period indicated. D-[^{3}H]Mannitol was used to estimate the extracellular trapping and nonspecific uptake of [^{14}C]TEA. Each point represents the mean ± S.D. for four to five slices from different rats. *, $p < 0.05$; ***, $p < 0.001$ versus sham-operated rats.

mRNA in I/R rat kidneys were significantly depressed to 48 and 4%, respectively.

Protein and mRNA Expression of rMATE1 in I/R-Induced AKI Rats. The effect of I/R-induced AKI on mRNA and protein expression of rMATE1 was examined. The rMATE1 protein level was markedly depressed in I/R rat kidneys (Fig. 5). As observed for the corresponding protein expression, the relative mRNA expression level of rMATE1 was significantly decreased in I/R rats (Fig. 5).

Discussion

Functional changes in renal organic ion transporters may be of clinical relevance, particularly to the use of drugs with high toxicity or a narrow therapeutic range. Serious kidney diseases, such as AKI, influence renal disposition of diverse organic ions in association with decreased glomerular filtration and function of transport systems. Our previous study demonstrated that the mRNA and protein expression levels of organic anion transporters, rOAT1 and rOAT3, were markedly suppressed with I/R-induced AKI, which was accompanied by significant elevation of the serum level of indoxyl sulfate, a uremic toxin that is a substrate of both rOAT1 and rOAT3 (Matsuzaki et al., 2007). In this study, we investigated the change in renal organic cation transporters, rOCT1, rOCT2, and rMATE1.

Three isoforms of organic cation transporter family members, OCT1, OCT2, and OCT3, were identified, and their physiological and pharmacokinetic roles have been evaluated (Inui et al., 2000; Jonker and Schinkel, 2004). rOCT1 is expressed abundantly in the liver and kidney (Gründemann et al., 1994), whereas rOCT2 is expressed predominantly in the kidney but not in the liver (Okuda et al., 1996). These transporters are localized to the basolateral membranes of renal proximal tubules. rOCT3 is expressed predominantly in the placenta but also has been detected in the intestine, heart, brain, lung, and very weakly in the kidney (Kekuda et al., 1998). In the renal proximal tubules of rats, rOCT1 and rOCT2 are considered to mediate the basolateral uptake of various cationic compounds. Previous reports suggested that the pharmacokinetics of famotidine are related to renal function (Manlucu et al., 2005). We found that the renal excretion of famotidine was significantly decreased in I/R rats (Fig. 1; Table 2). A transport study demonstrated that famotidine was a substrate for rOCT1, rOCT2, and rOAT3 (Tahara et al., 2005). Basolateral OCTs are known to be driven by the K^+-gradient associated with the inside-negative electrical potential difference, generated by Na^+/K^+-ATPase (Wright and Dantzler, 2004). We reported that

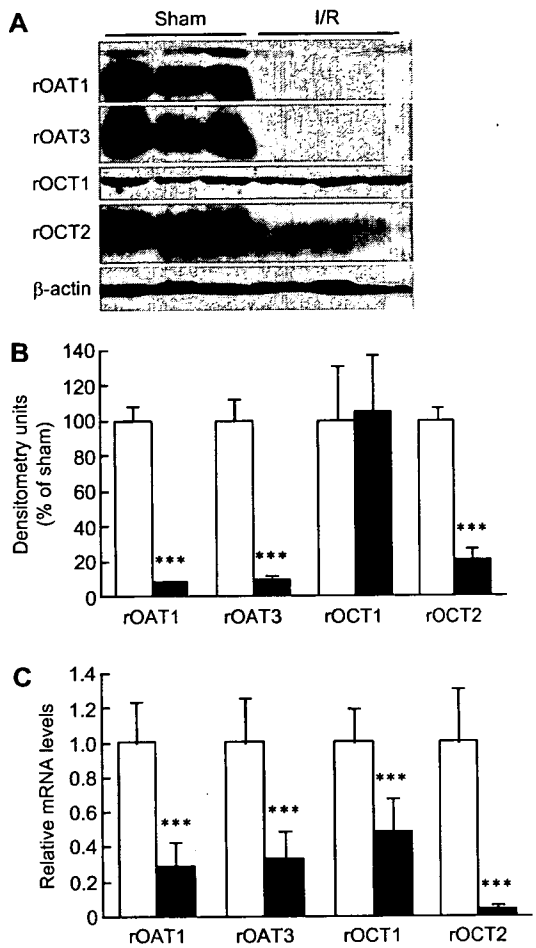

FIG. 4. Protein and mRNA expressions of basolateral organic ion transporters in the kidney of sham-operated and I/R rats. A, antisera specific for rOAT1, rOAT3, rOCT1, rOCT2, or β-actin were used as primary antibodies. B, ratio of rOAT1, rOAT3, rOCT1, and rOCT2 density to β-actin density in sham-operated (□) and I/R (■) rats. The values for sham-operated rats were arbitrarily defined as 100%. Each column represents the mean ± S.D. from three rats. C, mRNA expressions of basolateral organic ion transporters in the kidney of sham-operated and I/R rats. rOAT1, rOAT3, rOCT1, and rOCT2 mRNA expression levels in sham-operated (□) and I/R (■) rats were determined by real-time PCR analysis. The relative amounts of rOAT1, rOAT3, rOCT1, and rOCT2 mRNA were normalized to that of 18S ribosomal RNA. Each column represents the mean ± S.D. from seven to eight rats. ***, $p < 0.001$ versus sham-operated rats.

Na^+/K^+-ATPase expression was markedly depressed in the I/R rat kidney (Matsuzaki et al., 2007); thus, the driving force for OCTs at the basolateral membrane could be decreased in I/R rats. As shown in Figs. 2C and 3, organic cation transport activity at the basolateral membranes was reduced in I/R rat kidney, as the Kp value of TEA after i.v. administration and the accumulation of TEA into renal slices were significantly decreased to 20 and 36% of those in sham-operated rats, respectively. We reported previously that the transport activity of rOAT3 in I/R rats was significantly reduced to 52% of that in sham-operated rats, because the accumulation of estrone sulfate, a substrate of rOAT3, was decreased in renal slices from I/R rat kidney (Matsuzaki et al., 2007). It was reported that the Michaelis-Menten constant (K_m) values of famotidine for rOCT1, rOCT2, and rOAT3 were 87, 61, and 345 μM, respectively (Tahara et al., 2005). In this study, the estimated maximum plasma concentrations of famotidine in sham-operated and I/R rats were 154 and 148 μM, respectively. Considering the transporter affinity, decreased expression levels, and plasma concentration of famotidine in AKI rats, the decreased renal excretion of famotidine in I/R may be evoked mainly by the decreased

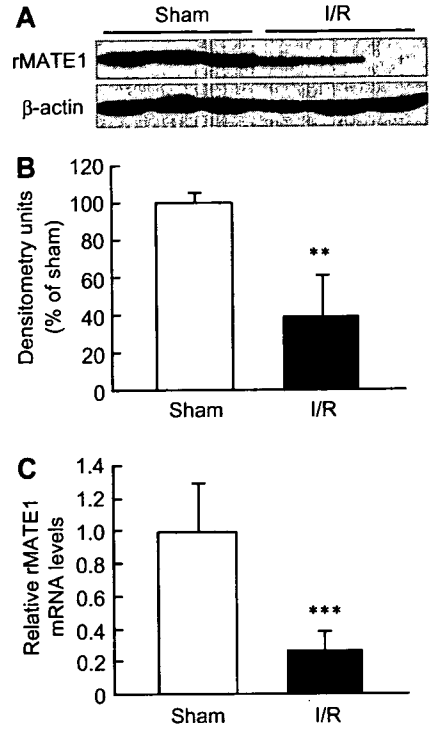

FIG. 5. Protein and mRNA expression of luminal rMATE1 in the kidney of sham-operated and I/R rats. A, antisera specific for rMATE1 or β-actin were used as primary antibodies. B, ratio of rMATE1 density to β-actin density in sham-operated and I/R rats. The values for sham-operated rats were arbitrarily defined as 100%. Each column represents the mean ± S.D. from three rats. C, mRNA expression of luminal rMATE1 in the kidney of sham-operated and I/R rats. rMATE1 mRNA expression levels were determined by real-time PCR analysis. The relative amount of rMATE1 mRNA was normalized to that of 18S ribosomal RNA. Each column represents the mean ± S.D. from seven to eight rats. **$p < 0.01$; ***, $p < 0.001$ versus sham-operated rats.

organic cation transport activity of the basolateral membrane in renal proximal tubules. Alternatively, the serum level of indoxyl sulfate, one of the high-affinity substrates for rOAT1 and rOAT3, was markedly elevated in I/R rats (Matsuzaki et al., 2007). Therefore, elevation of serum indoxyl sulfate could inhibit rOAT3 in a competitive manner, thereby decreasing renal accumulation of famotidine mediated by rOAT3.

Western blot analysis revealed that the expression of rOCT2, but not that of rOCT1, was significantly suppressed in I/R rat kidneys (Fig. 4). In addition, the mRNA expression of not only rOCT2 but also rOCT1 was significantly depressed (Fig. 4). The decrease in rOCT2 mRNA was remarkable compared with that in rOCT1 mRNA, suggesting that rOCT2 was more sensitive to I/R-induced AKI. Recently, it was reported that the expression of rOCT2 was decreased in rats with chronic renal failure (Ji et al., 2002), hyperuricemia (Habu et al., 2003), and diabetes mellitus (Thomas et al., 2004). Urakami et al. (2000) reported that the expression of rOCT2 was up-regulated by testosterone and down-regulated by estradiol in rats. It was also suggested that the lowered plasma level of testosterone was responsible for the decreased rOCT2 expression (Ji et al., 2002). Testosterone induces the expression of rOCT2 but not that of rOCT1 and rOCT3 via the androgen receptor-mediated transcriptional pathway (Asaka et al., 2006). However, it has been reported that there were no significant changes in plasma testosterone and estradiol after renal I/R-induced AKI (Park et al., 2004), although serum testosterone levels were decreased in bilateral ureteral ligation and uranyl nitrate or cisplatin-induced AKI (Ivic et al., 1988; Masubuchi et al., 2006). Therefore, further study on the factor(s) and mechanisms of the

decreased expression of rOCT2 is required to understand its regulation in AKI states.

In vivo renal clearances of famotidine and TEA were significantly decreased in I/R rats. Renal clearance of famotidine and TEA may be affected by organic cation transport activity not only at the basolateral membranes but also at the brush-border membranes, as renal secretion is performed by two transport steps in both membranes. In the rat renal tubular brush-border membranes, rMATE1 can mediate the organic cation transport energized by an inward-directed H^+ gradient, which is mainly generated by Na^+/H^+ exchanger (NHE) 3 (Moe, 1999). In five-sixths nephrectomized rats, the down-regulated expression of luminal rMATE1 was correlated well with the tubular secretion of cimetidine, and the expression of NHE3 was markedly depressed (Nishihara et al., 2007). TEA and cimetidine are substrates for rMATE1 (Ohta et al., 2006; Terada et al., 2006), although the ability of rMATE1 to recognize famotidine as a substrate is as yet unknown. We found that the protein and mRNA expressions of rMATE1 were markedly depressed in I/R rats (Fig. 5). Previously, it was reported that NHE3 expression was markedly depressed in I/R rats (Wang et al., 1997; Kwon et al., 2000), and the transport activity of organic cations in renal brush-border membranes was decreased in I/R rats (Maeda et al., 1993). Therefore, down-regulation of rMATE1 could be involved in the decreased renal clearance of TEA in I/R rats at the luminal membranes.

We have reported that I/R-induced AKI caused the down-regulation of basolateral rOCT2, accompanied by decreased organic cation transport activities at the basolateral membrane. Furthermore, luminal rMATE1 expression was markedly depressed in I/R rats, suggesting decreased organic cation transport activities at brush-border membranes. The present results suggest that the renal expressions of rOCT2 and rMATE1 are down-regulated and the urinary secretion of cationic drugs is decreased in AKI. Our findings provide information for understanding the mechanisms involved in pharmacokinetic alteration of drugs excreted mainly into urine under AKI, and the pathophysiological roles of basolateral rOCTs and luminal rMATE1.

References

Asaka J, Terada T, Okuda M, Katsura T, and Inui K (2006) Androgen receptor is responsible for rat organic cation transporter 2 gene regulation but not for rOCT1 and rOCT3. *Pharm Res* **23**:697–704.

Bonventre JV and Weinberg JM (2003) Recent advances in the pathophysiology of ischemic acute renal failure. *J Am Soc Nephrol* **14**:2199–2210.

Busch AE, Quester S, Ulzheimer JC, Waldegger S, Gorboulev V, Arndt P, Lang F, and Koepsell H (1996) Electrogenic properties and substrate specificity of the polyspecific rat cation transporter rOCT1. *J Biol Chem* **271**:32599–32604.

Cha SH, Sekine T, Fukushima JI, Kanai Y, Kobayashi Y, Goya T, and Endou H (2001) Identification and characterization of human organic anion transporter 3 expressing predominantly in the kidney. *Mol Pharmacol* **59**:1277–1286.

Gründemann D, Gorboulev V, Gambaryan S, Veyhl M, and Koepsell H. Drug excretion mediated by a new prototype of polyspecific transporter. *Nature* 372:549–552, 1994.

Habu Y, Yano I, Takeuchi A, Saito H, Okuda M, Fukatsu A, and Inui K (2003) Decreased activity of basolateral organic ion transports in hyperuricemic rat kidney: roles of organic ion transporters, rOAT1, rOAT3 and rOCT2. *Biochem Pharmacol* **66**:1107–1114.

Inui K, Masuda S, and Saito H (2000) Cellular and molecular aspects of drug transport in the kidney. *Kidney Int* **58**:944–958.

Ivi ć MA, Strahinjic S, Lajsic-Grubor G, and Stefanovic V (1988) Serum testosterone levels in experimental acute renal failure. *Exp Clin Endocrinol* **92**:349–356.

Ji L, Masuda S, Saito H, and Inui K (2002) Down-regulation of rat organic cation transporter rOCT2 by 5/6 nephrectomy. *Kidney Int* **62**:514–524.

Jonker JW and Schinkel AH (2004) Pharmacological and physiological functions of the polyspecific organic cation transporters: OCT1, 2, and 3 (SLC22A1–3). *J Pharmacol Exp Ther* **308**:2–9.

Kekuda R, Prasad PD, Wu X, Wang H, Fei YJ, Leibach FH, and Ganapathy V (1998) Cloning and functional characterization of a potential-sensitive, polyspecific organic cation transporter (OCT3) most abundantly expressed in placenta. *J Biol Chem* **273**:15971–15979.

Kwon TH, Frokiaer J, Han JS, Knepper MA, and Nielsen S (2000) Decreased abundance of major Na^+ transporters in kidneys of rats with ischemia-induced acute renal failure. *Am J Physiol* **278**:F925–F939.

Lin JH (1991) Pharmacokinetic and pharmacodynamic properties of histamine H_2-receptor antagonists: relationship between intrinsic potency and effective plasma concentrations. *Clin Pharmacokinet* **20**:218–236.

Maeda S, Takano M, Okano T, Ohoka K, Inui K, and Hori R (1993) Transport of organic cation in renal brush-border membrane from rats with renal ischemic injury. *Biochim Biophys Acta* **1150**:103–110.

Manlucu J, Tonelli M, Ray JG, Papaioannou A, Youssef G, Thiessen-Philbrook HR, Holbrook A, and Garg AX (2005) Dose-reducing H_2 receptor antagonists in the presence of low glomerular filtration rate: a systematic review of the evidence. *Nephrol Dial Transplant* 20:2376–2384.

Masubuchi Y, Kawasaki M, and Horie T (2006) Down-regulation of hepatic cytochrome P450 enzymes associated with cisplatin-induced acute renal failure in male rats. *Arch Toxicol* **80**:347–353.

Matsuzaki T, Watanabe H, Yoshitome K, Morisaki T, Hamada A, Nonoguchi H, Kohda Y, Tomita K, Inui K, and Saito H (2007) Downregulation of organic anion transporters in rat kidney under ischemia/reperfusion-induced acute renal failure. *Kidney Int* **71**:539–547.

Moe OW (1999) Acute regulation of proximal tubule apical membrane Na/H exchanger NHE-3: role of phosphorylation, protein trafficking, and regulatory factors. *J Am Soc Nephrol* **10**: 2412–2425.

Molitoris BA, Dahl R, and Geerdes A (1992) Cytoskeleton disruption and apical redistribution of proximal tubule Na^+-K^+-ATPase during ischemia. *Am J Physiol* **263**:F488–F495.

Nishihara K, Masuda S, Ji L, Katsura T, and Inui K (2007) Pharmacokinetic significance of luminal multidrug and toxin extrusion 1 in chronic renal failure rats. *Biochem Pharmacol* **73**:1482–1490.

Ohta KY, Inoue K, Hayashi Y, and Yuasa H (2006) Molecular identification and functional characterization of rat multidrug and toxin extrusion type transporter 1 as an organic cation/H^+ antiporter in the kidney. *Drug Metab Dispos* **34**:1868–1874.

Okuda M, Saito H, Urakami Y, Takano M, and Inui K (1996) cDNA cloning and functional expression of a novel rat kidney organic cation transporter, OCT2. *Biochem Biophys Res Commun* **224**:500–507.

Park KM, Kim JI, Ahn Y, Bonventre AJ, and Bonventre JV (2004) Testosterone is responsible for enhanced susceptibility of males to ischemic renal injury. *J Biol Chem* **279**:52282–52292.

Pritchard JB and Miller DS (1996) Renal secretion of organic anions and cations. *Kidney Int* **49**:1649–1654.

Schrier RW, Wang W, Poole B, and Mitra A (2004) Acute renal failure: definitions, diagnosis, pathogenesis, and therapy. *J Clin Invest* **114**:5–14.

Sekine T, Cha SH, and Endou H (2000) The multispecific organic anion transporter (OAT) family. *Pflugers Arch* **440**:337–350.

Sekine T, Watanabe N, Hosoyamada M, Kanai Y, and Endou H (1997) Expression cloning and characterization of a novel multispecific organic anion transporter. *J Biol Chem* **272**:18526–18529.

Star RA (1998) Treatment of acute renal failure. *Kidney Int* **54**:1817–1831.

Sweet DH and Pritchard JB (1999) The molecular biology of renal organic anion and organic cation transporters. *Cell Biochem Biophys* **31**:89–118.

Tahara H, Kusuhara H, Endou H, Koepsell H, Imaoka T, Fuse E, and Sugiyama Y (2005) A species difference in the transport activities of H_2 receptor antagonists by rat and human renal organic anion and cation transporters. *J Pharmacol Exp Ther* **315**:337–345.

Takano M, Inui K, Okano T, Saito H, and Hori R (1984) Carrier-mediated transport systems of tetraethylammonium in rat renal brush-border and basolateral membrane vesicles. *Biochim Biophys Acta* **773**:113–124.

Terada T, Masuda S, Asaka J, Tsuda M, Katsura T, and Inui K (2006) Molecular cloning, functional characterization and tissue distribution of rat H^+/organic cation antiporter MATE1. *Pharm Res* **23**:1696–1701.

Thadhani R, Pascual M, and Bonventre JV (1996) Acute renal failure. *N Engl J Med* **334**:1448–1460.

Thomas MC, Tikellis C, Kantharidis P, Burns WC, Cooper ME, and Forbes JM (2004) The role of advanced glycation in reduced organic cation transport associated with experimental diabetes. *J Pharmacol Exp Ther* **311**:456–466.

Tojo A, Sekine T, Nakajima N, Hosoyamada M, Kanai Y, Kimura K, and Endou H (1999) Immunohistochemical localization of multispecific renal organic anion transporter 1 in rat kidney. *J Am Soc Nephrol* **10**:464–471.

Ullrich KJ (1997) Renal transporters for organic anions and organic cations: structural requirements for substrates. *J Membr Biol* **158**:95–107.

Urakami Y, Okuda M, Masuda S, Akazawa M, Saito H, and Inui K (2001) Distinct characteristics of organic cation transporters, OCT1 and OCT2, in the basolateral membrane of renal tubules. *Pharm Res* **18**:1528–1534.

Urakami Y, Okuda M, Saito H, and Inui K (2000) Hormonal regulation of organic cation transporter OCT2 expression in rat kidney. *FEBS Lett* **473**:173–176.

Wang Z, Rabb H, Craig T, Burnham C, Shull GE, and Soleimani M (1997) Ischemic-reperfusion injury in the kidney: overexpression of colonic H^+-K^+-ATPase and suppression of NHE-3. *Kidney Int* **51**:1106–1115.

Wright SH and Dantzler WH (2004) Molecular and cellular physiology of renal organic cation and anion transport. *Physiol Rev* **84**:987–1049.

Address correspondence to: Dr. Hideyuki Saito, Department of Pharmacy, Kumamoto University Hospital, 1-1-1 Honjo, Kumamoto 860-8556, Japan. E-mail: saitohide@fc.kuh.kumamoto-u.ac.jp

BIOCHEMICAL PHARMACOLOGY XXX (2008) XXX–XXX

available at www.sciencedirect.com

ScienceDirect

journal homepage: www.elsevier.com/locate/biochempharm

Commentary

Physiological and pharmacokinetic roles of H^+/organic cation antiporters (MATE/SLC47A)☆

Tomohiro Terada, Ken-ichi Inui **

Department of Pharmacy, Kyoto University Hospital, Faculty of Medicine, Kyoto University, Sakyo-ku, Kyoto 606-8507, Japan

ARTICLE INFO

Keywords:
H^+/organic cation antiporter
Organic cation transporter
Renal tubular secretion
MATE1
MATE2-K
OCT

ABSTRACT

Vectorial secretion of cationic compounds across tubular epithelial cells is an important function of the kidney. This uni-directed transport is mediated by two cooperative functions, which are membrane potential-dependent organic cation transporters at the basolateral membranes and H^+/organic cation antiporters at the brush-border membranes. More than 10 years ago, the basolateral organic cation transporters (OCT1-3/SLC22A1-3) were isolated, and molecular understandings for the basolateral entry of cationic drugs have been greatly advanced. However, the molecular nature of H^+/organic cation antiport systems remains unclear. Recently, mammalian orthologues of the multidrug and toxin extrusion (MATE) family of bacteria have been isolated and clarified to function as H^+/organic cation antiporters. In this commentary, the molecular characteristics and pharmacokinetic roles of mammalian MATEs are critically overviewed focusing on the renal secretion of cationic drugs.

1. Introduction

The secretion of drugs and xenobiotics is an important physiological function of the renal proximal tubules. Transport studies using isolated membrane vesicles and cultured renal epithelial cells have suggested that the renal tubular secretion of cationic substances involves the concerted actions of two distinct classes of organic cation transporters: one facilitated by the transmembrane potential difference at the basolateral membranes and the other driven by the transmembrane H^+ gradient (H^+/organic cation antiporter) at the brush-border membranes [1–3]. A prototype substrate, tetraethylammonium (TEA), has been used for the functional characterization of these organic cation transport systems in the kidney.

The first membrane potential-dependent organic cation transporter (OCT1) was isolated from the rat kidney in 1994 [4]. Subsequently, we isolated rat (r) OCT2 cDNA [5]. Currently, there are three isoforms (OCT1-3/SLC22A1-3), and the physiological and pharmacokinetic roles of these transporters have been characterized from various standpoints. There are several excellent reviews documenting the historical developments and recent progress in the understanding of OCT families [6–10].

☆ This work was supported in part by the 21st Century Center of Excellence (COE) program "Knowledge Information Infrastructure for Genome Science", a Grant-in-Aid for Scientific Research from the Ministry of Education, Culture, Sports, Science and Technology of Japan, and a Grant-in-Aid for Research on Advanced Medical Technology from the Ministry of Health, Labor and Welfare of Japan.

* *Corresponding author.* Tel.: +81 75 751 3577; fax: +81 75 751 4207.
E-mail address: inui@kuhp.kyoto-u.ac.jp (K. Inui).

Abbreviations: MATE, multidrug and toxin extrusion; MPP, 1-methyl-4-phenylpyridinium; NMN, N^1-methylnicotinamide; OCT, organic cation transporter; OCTN, novel organic cation transporter; SLC, solute carrier; SNP, single nucleotide polymorphism; TEA, tetraethylammonium.

0006-2952/$ – see front matter © 2007 Elsevier Inc. All rights reserved.
doi:10.1016/j.bcp.2007.12.008

Please cite this article in press as: Terada T, Inui K, Physiological and pharmacokinetic roles of H^+/organic cation antiporters (MATE/SLC47A), Biochem Pharmacol (2008), doi:10.1016/j.bcp.2007.12.008

On the other hand, the molecular identification of H^+/organic cation antiport systems has not been progressed. Although several candidates for H^+/organic cation antiporters such as OCT2p [11], OCTN1 (SLC22A4) [12,13], and OCTN2 (SLC22A5) [14] have been proposed, all reports lacked direct and enough evidences to support the biochemical and physiological characteristics of H^+/organic cation antiport systems. For example, Tamai et al. [12] reported that OCTN1 may serve as a H^+/organic cation antiporter, because it can mediate the pH-dependent transport of TEA, and is localized at the brush-border membranes of renal proximal tubules. However, the following findings may not support that OCTN1 functions as classical H^+/organic cation antiport systems: (i) TEA transport by OCTN1 is electrogenic [13], whereas TEA transport by classical H^+/organic cation antiport systems is electroneutral [15], (ii) the renal expression level of OCTN1 is relatively weak [16], and (iii) OCTN1 has been demonstrated to mediate the Na^+-dependent transport of the fungal antioxidant, ergothioneine with much greater catalytic efficiency than for TEA [17,18]. Thus, no candidate fully satisfies the characteristics of H^+/organic cation antiport systems, and the true molecular nature of this transporter has been veiled for a long time.

2. Cloning of MATE/SLC47

In 1998, Tsuchiya and his colleagues [19] identified a novel multidrug transporter in *Vibrio parahaemolyticus* and its homolog in *Escherichia coli*, named NorM and YdhE, respectively. These two transporters were assigned to a new family of transporters designated as the multidrug and toxin extrusion (MATE) family [20]. Although the overall properties of the MATE family in bacteria have not been elucidated, some transporters mediated the H^+- or Na^+-coupled export of cationic drugs [20–22].

Based on these findings, Moriyama and his colleagues [23] searched for mammalian orthologues of MATE-type transporters using genomic databases, and succeeded in the isolation of cDNAs encoding orthologues of the bacterial MATE family, i.e., human (h) MATE1 (GenBank accession no. NP-060712), hMATE2 (NP-690872), mouse (m) MATE1 (AAH31436), and mMATE2 (XP-354611). Subsequently, we also reported the cDNA cloning of hMATE2-K (AB250364) [24], hMATE2-B (AB250701) [24], and rat (r) MATE1 (AB248823) [25]. Furthermore, other groups have reported the cloning of cDNAs for rMATE1 (AAH88413) [26], rabbit (rb) MATE1 (EF120627) [27], and rbMATE2-K (EF121852) [27]. The MATE family was assigned as the SLC47 family (SLC47A1: MATE1, SLC47A2: MATE2 and MATE2-K) by HUGO Gene Nomenclature Committee in 2007.

3. Concerns for nomenclature and classification

3.1. *hMATE2, hMATE2-K, and hMATE2-B*

During the course of our cloning process, the original hMATE2 cDNA could not be isolated, alternatively cDNAs for hMATE2-K and hMATE2-B were isolated [24]. As compared to the original hMATE2 cDNA, the hMATE2-K cDNA lacked 108 base pair (bp) in exon 7, and the hMATE2-B cDNA contained an insertion of 46 bp in exon 7. The open reading frame of the hMATE2-K cDNA was 1698 bp long, coding for a 566-amino acid protein. That of hMATE2-B was 660 bp long and encoded a 220-amino acid protein. hMATE2-K, but not hMATE2-B, exhibited the transport activity of TEA. Based on these findings, we originally described hMATE2-K as a splicing variant of hMATE2. However, subsequently, Zhang et al. [27] also isolated rbMATE2-K cDNA instead of rbMATE2 cDNA. So far, transport characteristics of the original hMATE2 remain unclear, whereas those of hMATE2-K and rbMATE2-K were clearly demonstrated [24,27,28]. Although the identification and characterization of the original hMATE2 should be carried out, MATE2-K is currently the only functional isoform in the MATE2 subfamily.

3.2. *mMATE2*

Moriyama's group classified rodent MATE2 (mMATE2 and rMATE2) as MATE3 family based on an amino acid alignment [29,30]. Dog, opossum and chimpanzee MATE3 are also members of MATE3 family [29,30]. This classification may be supported by tissue expression, i.e., human and rabbit MATE2-K are specifically expressed in the kidney, but rodent MATE2 is predominantly expressed in the testis [30]. In addition, based on the genomic database, it was found that there are no rodent isoforms corresponding to hMATE2-K. In order to avoid the misunderstanding of nomenclature, it would be reasonable to rename mMATE2 and rMATE2 as mMATE3 and rMATE3, respectively.

4. Structure

Human, mouse, rat, and rabbit MATE1 consists of 570, 532, 566, and 568 amino acid residues, respectively [23,25–27]. Phylogenetic trees of MATE1 and MATE2-K from various species are shown in Fig. 1A. A comparison of the multiple alignments of these MATE1 sequences revealed a similar overall homology except for the C-terminus of mMATE1 (Fig. 1B). Instead of the original mMATE1 (AAH31436, mMATE1a), another protein with 567 amino acid residues was registered in the NCBI database [CAI25734], which was recently reported as mMATE1b [31]. mMATE1b had almost the same C-terminal amino acid sequence as the other MATE1 proteins (Fig. 1B). In the cDNA of mMATE1b, a nucleotide 1528 "A" of the mMATE1a cDNA is deleted. mMATE1b has similar transport properties with mMATE1a and is localized at the renal brush-border membranes [31,32].

Hydropathy analysis in the original paper suggested that the hMATE1 protein contains 12 transmembrane domains, with both the C- and N-terminal located inside the cell. The secondary structure of various MATEs was examined by using transmembrane domain (TMD)-predicting programs such as SOSUI (http://sosui.proteome.bio.tuat.ac.jp/~sosui/proteome/sosuiframe0.html), TopPred (http://www.sbc.su.se/~erikw/toppred2/), TMHMM (http://www.cbs.dtu.dk/services/TMHMM-2.0/), and HMMTOP (http://www.enzim.hu/

Please cite this article in press as: Terada T, Inui K., Physiological and pharmacokinetic roles of H^+/organic cation antiporters (MATE/SLC47A), Biochem Pharmacol (2008), doi:10.1016/j.bcp.2007.12.008

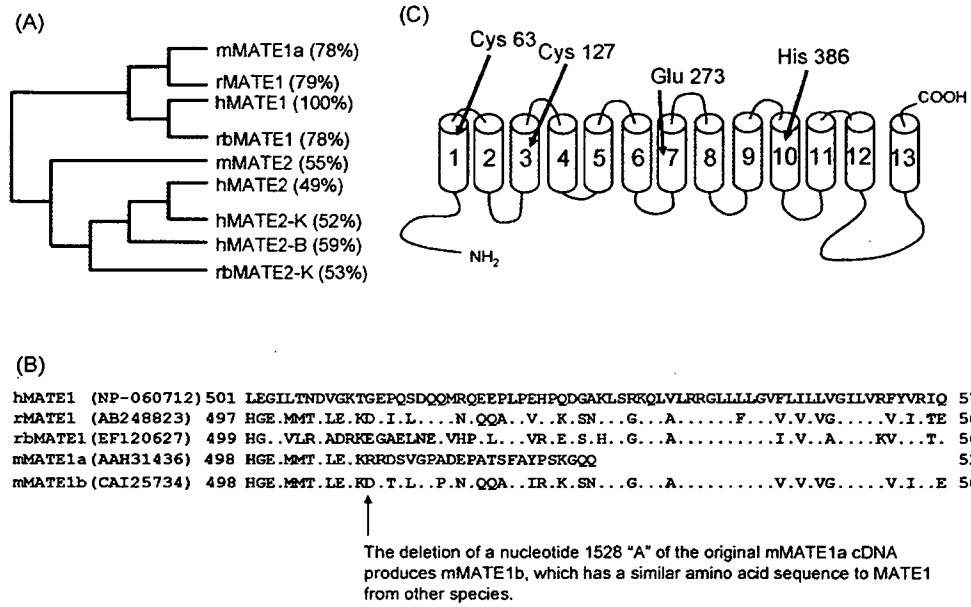

Fig. 1 – Structural characteristics of MATEs. (A) Phylogenetic trees of MATE1 and MATE2-K from various species. (B) Comparison of C-terminal amino acid sequence among the various MATE1 proteins. mMATE1b protein had almost the same C-terminal amino acid sequence as the other MATE1 proteins, but the original mMATE1a did not. (C) Secondary structure of hMATE1. Three different transmembrane domain-predicting programs suggested that hMATE1 has 13 transmembrane domains. Essential amino acid residues were identified by the mutagenesis analyses of hMATE1 [23,42].

hmmtop/html/document.html). Most of the programs suggested 13TMDs for the human, rat, and rabbit MATE1 (Fig. 1C), except for TopPred/hMATE1/12TMDs and SOSUI/rbMATE1/11TMDs. Twelve and 13 TMDs were predicted for the mMATE1a and mMATE1b, respectively. Thirteen TMDs would mean that the C-terminus of MATE proteins is located on the extracellular face of the membranes, and this orientation of rbMATE1 was confirmed by evaluating the accessibility of the antibody to a C-terminal tag using permeabilized and non-permeabilized cells [27].

Human and rabbit MATE2-K consists of 566 and 601 amino acid residues, respectively [24,27]. Most of the TMD-predicting programs also suggested that these proteins possessed 13 putative transmembrane domains like the MATE1 proteins.

5. Tissue distribution and membrane localization

hMATE1 mRNA is primarily expressed in the kidney, and is also expressed in the adrenal grand, testis, skeletal muscle and liver [23,24]. Immunohistochemical analyses showed the hMATE1 protein to be localized at the apical region of the proximal [23,24] and distal convoluted tubules [23] of the kidney.

rMATE1 is also strongly expressed in the kidney by Northern blot analyses [25,26]. Real-time PCR analyses revealed that rMATE1 mRNA is highly expressed in the kidney and placenta, and slightly expressed in the pancreas, spleen, bladder, and lung. Using micro-dissected nephron segments, it was demonstrated that rMATE1 mRNA was primarily expressed in the proximal convoluted tubule and proximal straight tubule, where expression levels of OCT1 and OCT2 are abundant. Immunohistochemical analyses also showed that rMATE1 was abundant in the renal cortex, and was detected at the brush-border membranes of proximal tubules [33].

mMATE1 mRNA was predominantly expressed in the kidney, liver, and heart as a 3.8-kb transcript by Northern blot analysis [23], and was also detected in the brain, heart, stomach, small intestine, urinary bladder, thyroid gland, adrenal gland, and testis as well as kidney and liver by RT-PCR analyses. In Western blot analysis, mMATE1 protein was detected as a single band of 53 kDa in the membranes of the kidney and liver [23], and also in the heart, stomach, small intestine, bladder, thyroid gland, adrenal gland, and testis [32]. Immunohistochemical analyses revealed that mMATE1 protein was localized not only at the apical region of proximal convoluted tubules and the bile canaliculi but also in brain glia-like cells and capillaries, pancreatic duct cells, urinary bladder epithelium, adrenal gland cortex, alpha cells of the islets of Langerhans, Leydig cells, and vitamin A-storing Ito cells [32]. It should be noted that the antibody used in these immunochemical analyses was raised against the C-terminus of the original mMATE1a [23,32]. The amino acid sequence of these regions of the original mMATE1a is completely different from that of mMATE1b [31] described in the section of structures. Although Hiasa et al. [32] suggested that mMATE1 mediates the transport of physiologically important cationic transmitters, steroids, and hormones in endocrine cells, the reevaluation of the tissue distribution and membrane localization of mMATE1b may be necessary to elucidate the physiological and pharmacokinetic roles of mMATE family.

hMATE2-K is expressed only in the kidney, and is localized at the brush-border membranes of the renal proximal tubules [24]. The precise tissue distribution of rbMATE2-K was not examined,

Please cite this article in press as: Terada T, Inui K., Physiological and pharmacokinetic roles of H^+/organic cation antiporters (MATE/SLC47A), Biochem Pharmacol (2008), doi:10.1016/j.bcp.2007.12.008

but the cortical expression of rbMATE2-K mRNA appeared to be approximately 7-fold that of rbMATE1 mRNA [27].

As described above, rodent MATE2 is classified into the third member of MATE family, and the sites of its expression are clearly different from those of hMATE2-K and rbMATE2-K. Rodent MATE2 is predominantly expressed in the testis, and is localized to the Leydig cells [23,30].

6. Functional aspects of MATEs

6.1. *Driving force*

MATE1 exhibited the pH-dependent transport of TEA in cellular uptake and efflux studies, and intracellular acidification through pretreatment with NH_4Cl stimulated TEA transport [23,25–28,31,32], suggesting that MATE1 utilized an oppositely directed H^+ gradient as a driving force. Uptake studies using plasma membrane vesicles from rMATE1-stably expressing cells definitively indicated that an oppositely directed H^+ gradient serves as a driving force for rMATE1 [34]. Namely, the transport of TEA exhibited the overshoot phenomenon only when there was an outwardly directed H^+ gradient, as observed in rat renal brush-border membrane vesicles (Fig. 2). The uptake of TEA stimulated by an H^+ gradient ($[H^+]_{in} > [H^+]_{out}$) was significantly reduced in the presence of a protonophore, carbonyl cyanide *p*-trifluoromethoxyphenylhydrazone (FCCP). TEA uptake stimulated by an H^+ gradient was not changed in the presence of valinomycin-induced membrane potential, suggesting the electroneutral antiport of H^+ and TEA. Since the luminal pH is more acidic than the intracellular pH in the proximal tubules [35], due to the Na^+/H^+ exchanger (NHE) and/or ATP-driven H^+-pump, it is reasonable to assume that the inward H^+ gradient (luminal pH < intracellular pH) can drive the secretion of organic cations in the kidney *in vivo*.

6.2. *Substrate specificity*

MATE1 and MATE2-K can transport typical organic cations such as TEA [23–28,31,32,34], H_2-blocker cimetidine [24–28,34], neurotoxin 1-methyl-4-phenylpyridinium (MPP) [24,25,27,28,34], and antiarrhythmic drug procainamide [24,25,28,34], all demonstrated to be substrates for H^+/organic cation antiporters characterized by brush-border membrane vesicles [1–3]. In addition to these compounds, N^1-methylnicotinamide (NMN), metformin (antidiabetic drug) and creatinine, which are cationic compounds, were transported by these transporters [24,25,28,34]. Zwitterionic β-lactam antibiotics such as cephalexin and cephradine are effectively transported by MATE1 [25,28], consistent with the results of transport experiments using rat renal brush-border membrane vesicles [36]. On the other hand, a platinum anticancer agent, oxaliplatin, was a better substrate for hMATE2-K rather than hMATE1 [37,38]. The pharmacokinetic implications of oxaliplatin transport via hMATE2-K are discussed below (Section 8). Though there are a few exceptions, substrate specificity of MATE1 and MATE2-K is similar in general. Furthermore, species differences regarding to substrate specificity have not been reported in MATE family among human, mouse, rat, and rabbit.

6.3. *Essential amino acid residues*

In the NorM protein, the prototype of the bacterial MATE family, three conserved acidic amino acid residues, Asp32, Glu251, and Asp367, in the transmembrane region were demonstrated to be involved in the Na^+-dependent drug transport process [39]. Glu273 in the human MATE1 protein, the counterpart of Glu251 of NorM, is also conserved among species, and Otsuka et al. [23] demonstrated that the mutation of Glu273 reduced the transport activity.

Our studies using rat renal brush-border membrane vesicles have suggested the functional importance of cysteine (Cys) and histidine (His) residues of the H^+/organic cation antiport system [40,41]. As expected, rMATE1 has Cys and His residues essential for the transport activities. Namely, among the conserved Cys and His residues of rMATE1, Cys62, Cys126, and His385 were identified as essential [42]. Mutation of the corresponding residues in hMATE1 and hMATE2-K also diminished the transport activity. The PCMBS-induced inhibition of TEA transport was protected by an excess of various rMATE1 substrates, suggesting that Cys residues act as substrate-binding sites. Pelis et al. [43] have recently found that Cys474 of hOCT2, suggested to be located in the 11th transmembrane

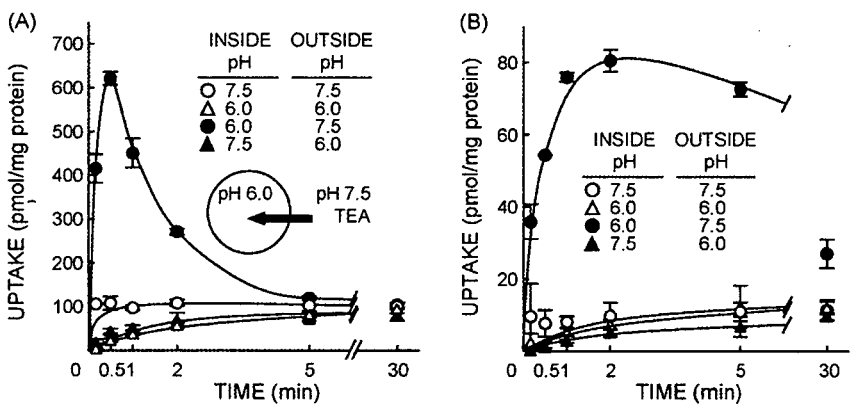

Fig. 2 – TEA uptake by rat renal brush-border membrane vesicles (A) and plasma membrane vesicles from rat MATE1-stably expressing cells (B). The transport of TEA exhibited the overshoot phenomenon only when there was an outwardly directed H^+ gradient in both systems.

Please cite this article in press as: Terada T, Inui K. Physiological and pharmacokinetic roles of H^+/organic cation antiporters (MATE/SLC47A). Biochem Pharmacol (2008), doi:10.1016/j.bcp.2007.12.008

helix which participates in the formation of the hydrophilic cleft, contributes to substrate–protein interaction. As OCTs and MATEs have similar substrate specificity, even if their driving forces are different, it is plausible that the same amino acid cysteine is involved in the recognition of substrates.

7. Regulational aspects of MATEs

7.1. *Comparison with OCTs*

In the case of the basolateral organic cation transporters (OCTs), it has been reported that various factors such as development [44], gender [45,46], chronic renal failure after 5/6 nephrectomy [47], and diabetes [48] affected the expression of OCTs in the kidney. For example, the expression level of rat OCT2, but not OCT1 or OCT3, in the kidney was much higher in males than females [45]. The treatment of male and female rats with testosterone significantly increased rOCT2 expression in the kidney [46]. Indeed, functional reporter assays revealed that androgen response elements in the rat OCT2 promoter region play important roles in the enhancement of transcription by testosterone [49]. Recently, as a basal transcriptional regulator of the hOCT2 gene, upstream stimulatory factor 1 was identified [50].

In contrast to OCTs, there is little information available about the regulation of MATEs, and similar approaches for MATEs have been carried out. A gender difference was not observed in rMATE1 protein [33] and rbMATE1 and rbMATE2-K mRNA [27]. The level of basolateral rOCT2 was changed in male nephrectomized rats, but was not changed in female nephrectomized rats [33]. Based on these findings, female rats were used to evaluate the roles of luminal rMATE1 in nephrectomized rats, avoiding the influence of basolateral side [33]. The tubular secretion of cimetidine was markedly decreased in female nephrectomized rats. Although the protein expression of rOCT2 was not changed, the level of rMATE1 was significantly decreased in the remnant kidney. The protein level of rMATE1, but not of rOCT2, correlated well with the tubular secretion of cimetidine. The level of NHE3 was also markedly depressed in both the male and female nephrectomized rats. These results suggested that the secretion of cimetidine was decreased by the reduced expression of rMATE1 but also by the functional loss of this transporter due to a lowered H^+-gradient at the brush-border membrane, caused by a decrease in NHE3.

7.2. *Promoter and rSNP analyses of the MATE1 gene*

Functional promoter analyses of the human and rat MATE1 genes were recently characterized [51]. Deletion analyses suggested that the region spanning −65/−25 was essential for the basal transcriptional activity of human MATE1, and this region lacked a canonical TATA box, but possessed two putative Sp1-binding sites. The functional involvement of Sp1 was confirmed by the overexpression of Sp1, a mutational analysis of Sp1-binding sites, mithramycin A treatment, and an electrophoretic mobility shift assay. Interestingly, a single nucleotide polymorphism (SNP) was discovered in the Sp1-binding site (G-32A) of the hMATE1 promoter, and it was

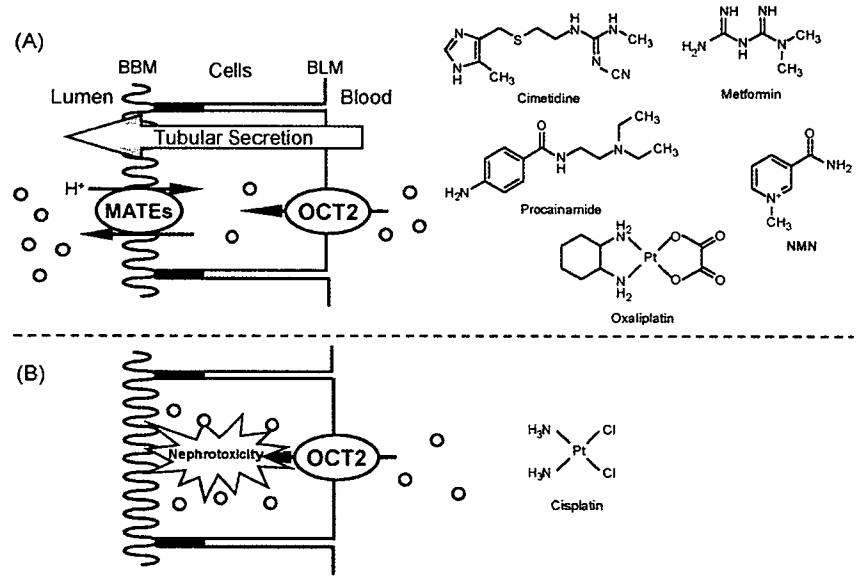

Fig. 3 – Organic cation transport systems in human renal proximal tubular cells and chemical structures of typical substrates. Cellular uptake of organic cations across the basolateral membranes (BLM) is mediated by membrane potential-dependent organic cation transporter 2 (OCT2). In human proximal tubular cells, there is little expression of other isoforms such as OCT1 and OCT3. The exit of cellular organic cations across the brush-border membranes (BBM) is mediated principally by H^+/organic cation antiporters (MATE1 and MATE2-K). (A) Cimetidine, metformin, procainamide, and NMN recognized by both transporters are mainly excreted into the urine. Oxaliplatin is transported by both transporters, and could not be accumulated in the renal proximal tubular cells. (B) Cisplatin is transported by hOCT2, but not by hMATE family. These transport properties may induce the accumulation of cisplatin in the renal proximal tubular cells and nephrotoxicity.

Please cite this article in press as: Terada T, Inui K., Physiological and pharmacokinetic roles of H^+/organic cation antiporters (MATE/SLC47A), Biochem Pharmacol (2008), doi:10.1016/j.bcp.2007.12.008

Table 1 – Characteristics of MATE family

	hMATE1/SLC47A1 [23,24,28,37,38,42,51]	hMATE2-K/SLC47A2 [24,28,37,38,42]	MATEs of other species [23,25–27,30–34,38,42,51]
Amino acids	570	566	566 (r), 532 (m1a), 567 (m1b), 573 (m2), 568 (rb1), 601 (rb2-K)
Tissue distribution	Kidney, adrenal grand ≫ testis > skeletal muscle, liver, uterus	Kidney	Kidney, placenta > pancreas, spleen, bladder, lung (r); kidney, liver, brain, heart, stomach, small intestine, urinary bladder, thyroid gland, adrenal gland, testis (m1a); kidney (m1b, rb1, rb2-K); testis (m2)
Membrane localization	Brush-border membranes	Brush-border membranes	Brush-border membranes
Driving force	Oppositely directed H^+ gradient	Oppositely directed H^+ gradient	Oppositely directed H^+ gradient
Substrates	TEA, cimetidine, MPP, procainamide, metformin, creatinine, cephalexin, cephradine, etc.	TEA, cimetidine, MPP, procainamide, NMN, metformin, creatinine, oxaliplatin, etc.	TEA (r, m1a, m1b, m2, rb1, rb2-K), cimetidine (r, rb1, rb2-K), MPP (r, rb1, rb2-K), procainamide (r), NMN (r), metformin (r), creatinine (r), cephalexin (r), oxaliplatin (r), etc.
Essential amino acid residues	Cys63, Cys127, Glu273, His386	Cys59, Cys123, His382	Cys62 (r), Cys126 (r), His385 (r)
Transcription factor	Sp1	Sp1	Sp1 (r)

The abbreviations in the MATEs of other species are as follows: r, rat MATE1; m1a, mouse MATE1a; m1b, mouse MATE1b; m2, mouse MATE2; rb1, rabbit MATE1; rb2-K, rabbit MATE2-K.

demonstrated that this substitution affects hMATE1 promoter activity by disrupting the binding of Sp1 (an approximately 50% reduction relative to the control), suggesting that this SNP influences the mRNA level of MATE1.

To date, many large-scale screenings of SNPs of SLC drug transporters have been carried out to identify genetic factors involved in the interindividual differences of pharmacokinetics. Recently, it has been demonstrated that OCT1 genotype is a determinant of the therapeutic action and pharmacokinetics of metformin [52,53]. Because MATE1 plays pivotal roles in the renal handling of metformin, the SNP in the promoter region of the *MATE1* gene may affect the pharmacokinetic properties of metformin. Further studies of the relationship between gene polymorphisms of MATE1 and the pharmacokinetics of MATE1 substrate drugs including metformin may clarify the clinical implications of this SNP.

8. Pharmacokinetic and toxicological roles

In general, efficient renal secretion of organic cations could be achieved by the efficient interplay between OCT2 and MATE1 and/or MATE2-K in human renal tubular epithelial cells. Cationic drugs such as cimetidine, metformin, and procainamide, and endogenous organic cations such as NMN recognized by both transporters were mainly excreted into the urine (Fig. 3A). These transporters also control the exposure of renal cells to nephrotoxic drugs and thereby are responsible for xenobiotic-induced nephrotoxicity.

Cisplatin, carboplatin, oxaliplatin, and nedaplatin are currently used to treat solid tumors. Among them, only cisplatin induces nephrotoxicity with a higher accumulation in the kidney. *In vitro* and *in vivo* studies indicated that a kidney-specific OCT2 was the determinant of cisplatin-induced nephrotoxicity, mediating the renal uptake of cisplatin [37,54]. In addition, low-nephrotoxic platinum agents, carboplatin and nedaplatin, were not transported by OCT2. However, oxaliplatin was revealed to be a good substrate of OCT2 although it was not nephrotoxic. We hypothesized that hMATE1 and/or hMATE2-K protect against oxaliplatin-induced nephrotoxicity by effluxing this agent from the intracellular compartment. As expected, marked transport of oxaliplatin by hMATE2-K, but not hMATE1, was observed [37,38]. On the other hand, cisplatin, carboplatin, and nedaplatin were not transported by either transporter [37,38]. These results clearly account for the relationship between the renal pharmacokinetics and nephrotoxicity of platinum agents; (i) cisplatin was accumulated in the kidney via hOCT2 and induced nephrotoxicity (Fig. 3B), (ii) oxaliplatin was transported by hMATE2-K as well as hOCT2 and therefore, its renal cellular concentration was lowered (Fig. 3A), and (iii) carboplatin and nedaplatin were not accumulated in the kidney via organic cation transporters. The MATE family is proposed to play an important role in protecting the kidney from cationic toxins.

9. Summary and perspective

In this commentary, we described recent findings about the MATE/SLC47A family regarding their structure, expression,

Please cite this article in press as: Terada T, Inui K-, Physiological and pharmacokinetic roles of H^+/organic cation antiporters (MATE/SLC47A), Biochem Pharmacol (2008), doi:10.1016/j.bcp.2007.12.008

transport function, and regulation (Table 1). Most of the molecular characteristics of MATEs are consistent with the biochemical properties of renal H^+/organic cation antiport systems assessed by classical assays using *in vitro* brush-border membrane vesicles and cultured renal epithelial cells. With respect to the roles of MATEs, their pharmacokinetic significance including renal secretion has been emphasized. In human proximal tubular cells, the renal tubular secretion of clinically important cationic drugs is mediated by the interplay of basolateral OCT2 and brush-border MATE1/MATE2-K (Fig. 3). Thus, the establishment of OCT/MATE double transfectants could be useful for the evaluation and prediction for the renal handling of cationic drugs, drug–drug interactions, and drug toxicity. Although there is little information available about the regulational aspects of MATEs, similar evidences have been accumulated for other renal drug transporters [55]. An understanding of the mechanisms for the regulation of MATEs will help us to evaluate the intra- and interindividual variability in the renal handling of cationic drugs. Finally, regarding the classification of the mammalian MATE family, we recommend that mouse and rat MATE2 could be renamed mouse and rat MATE3, respectively.

REFERENCES

[1] Inui K, Takano M, Hori R. Organic cation transport in the renal brush-border and basolateral membranes. In: Hatano M, editor. Nephrology. Tokyo: Springer-Verlag; 1991. p. 1391–8.
[2] Pritchard JB, Miller DS. Mechanisms mediating renal secretion of organic anions and cations. Physiol Rev 1993;73:765–96.
[3] Inui K, Okuda M. Cellular and molecular mechanisms of renal tubular secretion of organic anions and cations. Clin Exp Nephrol 1998;2:100–8.
[4] Gründemann D, Gorboulev V, Gambaryan S, Veyhl M, Koepsell H. Drug excretion mediated by a new prototype of polyspecific transporter. Nature 1994;372:549–52.
[5] Okuda M, Saito H, Urakami Y, Takano M, Inui K. cDNA cloning and functional expression of a novel rat kidney organic cation transporter, OCT2. Biochem Biophys Res Commun 1996;224:500–7.
[6] Inui K, Masuda S, Saito H. Cellular and molecular aspects of drug transport in the kidney. Kidney Int 2000;58:944–58.
[7] Burckhardt G, Wolff NA. Structure of renal organic anion and cation transporters. Am J Physiol Renal Physiol 2000;278:F853–66.
[8] Jonker JW, Schinkel AH. Pharmacological and physiological functions of the polyspecific organic cation transporters: OCT1, 2, and 3 (SLC22A1-3). J Pharmacol Exp Ther 2004;308:2–9.
[9] Wright SH. Role of organic cation transporters in the renal handling of therapeutic agents and xenobiotics. Toxicol Appl Pharmacol 2005;204:309–19.
[10] Koepsell H, Lips K, Volk C. Polyspecific organic cation transporters: structure, function, physiological roles, and biopharmaceutical implications. Pharm Res 2007;24:1227–51.
[11] Gründemann D, Babin-Ebell J, Martel F, Ording N, Schmidt A, Schömig E. Primary structure and functional expression of the apical organic cation transporter from kidney epithelial LLC-PK_1 cells. J Biol Chem 1997;272:10408–13.
[12] Tamai I, Yabuuchi H, Nezu J, Sai Y, Oku A, Shimane M, et al. Cloning and characterization of a novel human pH-dependent organic cation transporter, OCTN1. FEBS Lett 1997;419:107–11.
[13] Tamai I, Nakanishi T, Kobayashi D, China K, Kosugi Y, Nezu J, et al. Involvement of OCTN1 (SLC22A4) in pH-dependent transport of organic cations. Mol Pharm 2004;1:57–66.
[14] Ohashi R, Tamai I, Nezu J, Nikaido H, Hashimoto N, Oku A, et al. Molecular and physiological evidence for multifunctionality of carnitine/organic cation transporter OCTN2. Mol Pharmacol 2001;59:358–66.
[15] Takano M, Inui K, Okano T, Saito H, Hori R. Carrier-mediated transport systems of tetraethylammonium in rat renal brush-border and basolateral membrane vesicles. Biochim Biophys Acta 1984;773:113–24.
[16] Motohashi H, Sakurai Y, Saito H, Masuda S, Urakami Y, Goto M, et al. Gene expression levels and immunolocalization of organic ion transporters in the human kidney. J Am Soc Nephrol 2002;13:866–74.
[17] Gründemann D, Harlfinger S, Golz S, Geerts A, Lazar A, Berkels R, et al. Discovery of the ergothioneine transporter. Proc Natl Acad Sci USA 2005;102:5256–61.
[18] Grigat S, Harlfinger S, Pal S, Striebinger R, Golz S, Geerts A, et al. Probing the substrate specificity of the ergothioneine transporter with methimazole, hercynine, and organic cations. Biochem Pharmacol 2007;74:309–16.
[19] Morita Y, Kodama K, Shiota S, Mine T, Kataoka A, Mizushima T, et al. NorM, a putative multidrug efflux protein, of Vibrio parahaemolyticus and its homolog in *Escherichia coli*. Antimicrob Agents Chemother 1998;42:1778–82.
[20] Brown MH, Paulsen IT, Skurray RA. The multidrug efflux protein NorM is a prototype of a new family of transporters. Mol Microbiol 1999;31:394–5.
[21] Putman M, van Veen HW, Konings WN. Molecular properties of bacterial multidrug transporters. Microbiol Mol Biol Rev 2000;64:672–93.
[22] Hvorup RN, Winnen B, Chang AB, Jiang Y, Zhou XF, Saier Jr MH. The multidrug/oligosaccharidyl-lipid/polysaccharide (MOP) exporter superfamily. Eur J Biochem 2003;270:799–813.
[23] Otsuka M, Matsumoto T, Morimoto R, Arioka S, Omote H, Moriyama Y. A human transporter protein that mediates the final excretion step for toxic organic cations. Proc Natl Acad Sci USA 2005;102:17923–8.
[24] Masuda S, Terada T, Yonezawa A, Tanihara Y, Kishimoto K, Katsura T, et al. Identification and functional characterization of a new human kidney-specific H^+/organic cation antiporter, kidney-specific multidrug and toxin extrusion 2. J Am Soc Nephrol 2006;17:2127–35.
[25] Terada T, Masuda S, Asaka J, Tsuda M, Katsura T, Inui K. Molecular cloning, functional characterization and tissue distribution of rat H^+/organic cation antiporter MATE1. Pharm Res 2006;23:1696–701.
[26] Ohta KY, Inoue K, Hayashi Y, Yuasa H. Molecular identification and functional characterization of rat multidrug and toxin extrusion type transporter 1 as an organic cation/H^+ antiporter in the kidney. Drug Metab Dispos 2006;34:1868–74.
[27] Zhang X, Cherrington NJ, Wright SH. Molecular identification and functional characterization of rabbit MATE1 and MATE2-K. Am J Physiol Renal Physiol 2007;293:F360–70.
[28] Tanihara Y, Masuda S, Sato T, Katsura T, Ogawa O, Inui K. Substrate specificity of MATE1 and MATE2-K, human multidrug and toxin extrusions/H^+-organic cation antiporters. Biochem Pharmacol 2007;74:359–71.
[29] Omote H, Hiasa M, Matsumoto T, Otsuka M, Moriyama Y. The MATE proteins as fundamental transporters of

Please cite this article in press as: Terada T, Inui K., Physiological and pharmacokinetic roles of H^+/organic cation antiporters (MATE/SLC47A), Biochem Pharmacol (2008), doi:10.1016/j.bcp.2007.12.008

metabolic and xenobiotic organic cations. Trends Pharmacol Sci 2006;27:587–93.
[30] Hiasa M, Matsumoto T, Komatsu T, Omote H, Moriyama Y. Functional characterization of testis-specific rodent multidrug and toxic compound extrusion 2 (MATE2) a class III MATE-type H^+/organic cation exporter. Am J Physiol Cell Physiol 2007;293:C1437–44.
[31] Kobara A, Hiasa M, Matsumoto T, Otsuka M, Omote H, Moriyama Y. A novel variant of mouse MATE-1 H+/organic cation antiporter with a long hydrophobic tail. Arch Biochem Biophys 2008;469:195–9.
[32] Hiasa M, Matsumoto T, Komatsu T, Moriyama Y. Wide variety of locations for rodent MATE1, a transporter protein that mediates the final excretion step for toxic organic cations. Am J Physiol Cell Physiol 2006;291:C678–86.
[33] Nishihara K, Masuda S, Ji L, Katsura T, Inui K. Pharmacokinetic significance of luminal multidrug and toxin extrusion 1 in chronic renal failure rats. Biochem Pharmacol 2007;73:1482–90.
[34] Tsuda M, Terada T, Asaka J, Ueba M, Katsura T, Inui K. Oppositely directed H^+ gradient functions as a driving force of rat H^+/organic cation antiporter MATE1. Am J Physiol Renal Physiol 2007;292:F593–8.
[35] Yoshitomi K, Fromter E. Cell pH of rat renal proximal tubule in vivo and the conductive nature of peritubular HCO_3^- (OH^-) exit. Pflügers Arch 1984;402:300–5.
[36] Inui K, Takano M, Okano T, Hori R. H^+ gradient-dependent transport of aminocephalosporins in rat renal brush border membrane vesicles: role of H^+/organic cation antiport system. J Pharmacol Exp Ther 1985;233:181–5.
[37] Yonezawa A, Masuda S, Yokoo S, Katsura T, Inui K. Cisplatin and oxaliplatin, but not carboplatin and nedaplatin, are substrates for human organic cation transporters (SLC22A1-3 and multidrug and toxin extrusion family). J Pharmacol Exp Ther 2006;319:879–86.
[38] Yokoo S, Yonezawa A, Masuda S, Fukatsu A, Katsura T, Inui K. Differential contribution of organic cation transporters, OCT2 and MATE1, in platinum agent-induced nephrotoxicity. Biochem Pharmacol 2007;74:477–87.
[39] Otsuka M, Yasuda M, Morita Y, Otsuka C, Tsuchiya T, Omote H, et al. Identification of essential amino acid residues of the NorM Na^+/multidrug antiporter in Vibrio parahaemolyticus. J Bacteriol 2005;187:1552–8.
[40] Hori R, Maegawa H, Kato M, Katsura T, Inui K. Inhibitory effect of diethyl pyrocarbonate on the H^+/organic cation antiport system in rat renal brush-border membranes. J Biol Chem 1989;264:12232–7.
[41] Hori R, Maegawa H, Okano T, Takano M, Inui K. Effect of sulfhydryl reagents on tetraethylammonium transport in rat renal brush border membranes. J Pharmacol Exp Ther 1987;241:1010–6.
[42] Asaka J, Terada T, Tsuda M, Katsura T, Inui K. Identification of essential histidine and cysteine residues of the H^+/organic cation antiporter multidrug and toxin extrusion (MATE). Mol Pharmacol 2007;71:1487–93.
[43] Pelis RM, Zhang X, Dangprapai Y, Wright SH. Cysteine accessibility in the hydrophilic cleft of human organic cation transporter 2. J Biol Chem 2006;281:35272–80.
[44] Pavlova A, Sakurai H, Leclercq B, Beier DR, Yu AS, Nigam SK. Developmentally regulated expression of organic ion transporters NKT (OAT1), OCT1, NLT (OAT2), and Roct. Am J Physiol Renal Physiol 2000;278:F635–43.
[45] Urakami Y, Nakamura N, Takahashi K, Okuda M, Saito H, Hashimoto Y, et al. Gender differences in expression of organic cation transporter OCT2 in rat kidney. FEBS Lett 1999;461:339–42.
[46] Urakami Y, Okuda M, Saito H, Inui K. Hormonal regulation of organic cation transporter OCT2 expression in rat kidney. FEBS Lett 2000;473:173–6.
[47] Ji L, Masuda S, Saito H, Inui K. Down-regulation of rat organic cation transporter rOCT2 by 5/6 nephrectomy. Kidney Int 2002;62:514–24.
[48] Thomas MC, Tikellis C, Burns WC, Thallas V, Forbes JM, Cao Z, et al. Reduced tubular cation transport in diabetes: prevented by ACE inhibition. Kidney Int 2003;63:2152–61.
[49] Asaka J, Terada T, Okuda M, Katsura T, Inui K. Androgen receptor is responsible for rat organic cation transporter 2 gene regulation but not for rOCT1 and rOCT3. Pharm Res 2006;23:697–704.
[50] Asaka J, Terada T, Ogasawara K, Katsura T, Inui K. Characterization of the basal promoter element of human organic cation transporter 2 gene. J Pharmacol Exp Ther 2007;321:684–9.
[51] Kajiwara M, Terada T, Asaka J, Ogasawara K, Katsura T, Ogawa O, et al. Critical roles of Sp1 in gene expression of human and rat H^+/organic cation antiporters (MATE1). Am J Physiol Renal Physiol 2007;293:F1564–70.
[52] Shu Y, Sheardown SA, Brown C, Owen RP, Zhang S, Castro RA, et al. Effect of genetic variation in the organic cation transporter 1 (OCT1) on metformin action. J Clin Invest 2007;117:1422–31.
[53] Shu Y, Brown C, Castro RA, Shi RJ, Lin ET, Owen RP, et al. Effect of genetic variation in the organic cation transporter 1, OCT1, on metformin pharmacokinetics. Clin Pharmacol Ther 2008;83:273–80.
[54] Yonezawa A, Masuda S, Nishihara K, Yano I, Katsura T, Inui K. Association between tubular toxicity of cisplatin and expression of organic cation transporter rOCT2 (Slc22a2) in the rat. Biochem Pharmacol 2005;70:1823–31.
[55] Terada T, Inui K. Gene expression and regulation of drug transporters in the intestine and kidney. Biochem Pharmacol 2007;73:440–9.

Please cite this article in press as: Terada T, Inui K. Physiological and pharmacokinetic roles of H^+/organic cation antiporters (MATE/SLC47A). Biochem Pharmacol (2008), doi:10.1016/j.bcp.2007.12.008